

Woods Hole Oceanographic Institution



Extracting Wind Sea and Swell from Directional Wave Spectra Derived from a Bottom-Mounted ADCP

by

James H. Churchill,
Albert J. Plueddemann,
and Stephen M. Faluotico

Woods Hole Oceanographic Institution
Woods Hole, MA 02543

July 2006

Technical Report

Funding was provided by the Office of Naval Research under Contract No. N00014-03-1-0681.

Approved for public release; distribution unlimited.

WHOI-2006-13

**Extracting Wind Sea and Swell from Directional Wave Spectra Derived from a
Bottom-Mounted ADCP**

by

James H. Churchill,
Albert J. Plueddemann,
and Stephen M. Faluotico

July 2006

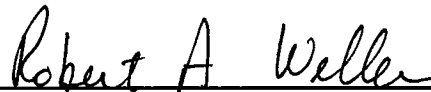
Technical Report

Funding was provided by the Office of Naval Research under Contract No. N00014-03-1-0681.

Reproduction in whole or in part is permitted for any purpose of the United States Government. This report should be cited as Woods Hole Oceanog. Inst. Tech. Rept., WHOI-2006-13.

Approved for public release; distribution unlimited.

Approved for Distribution:



Robert A. Weller, Chair

Department of Physical Oceanography

Abstract

Recent advances in processing velocity data from bottom-mounted Acoustic Doppler Current Profilers (ADCPs) offer the capability of partitioning directional wave spectra of surface wave height in order to separate the locally generated wind waves from incoming swells arriving from remote sources. In the study described here, we have partitioned directional wave spectra, derived from bottom-mounted ADCP measurements at the Martha's Vineyard Coastal Observatory (MVCO) south of Martha's Vineyard, MA, into dominant swell and locally generated wind-wave components. The partitioning was carried out following the method of Hanson and Phillips (2001). Because this is a relatively untested method, especially when applied to ADCP data, it was implemented by an exploratory, rather than a routine, approach. As part of this approach, we assessed the validity of the ADCP-derived wave spectra by comparing them with one-dimensional wave spectra derived from laser altimeter measurements. As will be shown, this comparison identified a frequency range over which the ADCP-derived wave field may be suspect. We also carried out a series of sensitivity tests in which we evaluated how the results of wave partitioning according to the Hanson and Phillips (2001) method is influenced by varying the parameters required to implement the method. In this report, we describe and assess the data sources used in our study, outline the methods employed for wave spectra partitioning and describe partitioning results (focusing on the sensitivity of these results to the partitioning parameters).

Table of Contents

Abstract	iii
List of Figures	v
List of Tables	v
1. Introduction.....	1
2. Data Sources and Data Processing.....	1
a. Wind Velocity	1
b. Laser Altimeter-Derived Wave Spectra.....	4
c. ADCP-Derived Wave Spectra	5
d. Comparison of ADCP- and Laser Altimeter-Derived Wave Spectra	5
3. Wave Spectra Partitioning	7
a. Wind Sea Identification	7
b. APL-WAVES Parameters	8
4. Results	9
a. Parameter Sensitivity Tests	9
c. Output of Spectral Partitioning	25
Acknowledgments.....	32
References.....	33
Appendix 1. Description of Output Variables	34

List of Figures

Figure 1. MVCO site map.....	2
Figure 2. Comparison of 10 m wind records	3
Figure 3. Scatter plot of 10 m wind velocities.....	4
Figure 4. Comparison of 1-dimensional spectra	6
Figure 5. Comparison of time-averaged frequency spectra	7
Figure 6. Example of directional wave spectrum, 28 Aug 21:20	10
Figure 7. Example of directional wave spectrum, 29 Aug 03:20	11
Figure 8. Partitioned wave-field statistics, parameter set a	14
Figure 9. Partitioned wave-field statistics, parameter set b	15
Figure 10. Partitioned wave-field statistics, parameter set c	16
Figure 11. Partitioned wave-field statistics, parameter set d	17
Figure 12. Partitioned wave-field statistics, parameter set e	18
Figure 13. Partitioned wave-field statistics, parameter set f	19
Figure 14. Partitioned wave-field statistics, parameter set g	20
Figure 15. Partitioned wave-field statistics, parameter set h	21
Figure 16. Partitioned wave-field statistics, parameter set i	22
Figure 17. Comparison of partitioning results, 29 Aug 03:00	23
Figure 18. Comparison of partitioning results, 29 Aug 10:00	24
Figure 19. Wave properties for year day 211-240	27
Figure 20. Wave properties for year day 241-270	28
Figure 21. Wave properties for year day 271-300	29
Figure 22. Wave properties for year day 301-330	30
Figure 23. Wave properties for year day 331-360	31

List of Tables

Table 1. Measurement locations	3
Table 2. Parameter sets used in sensitivity tests	12

1. Introduction

A coastal wave field often presents an observer with complex patterns created by the interaction of locally generated wind waves with swells from a distant source, or sources. Recent advances in processing data from bottom-mounted ADCPs offer the capability of partitioning directional wave spectra of surface wave height, separating the locally-generated wind waves from incoming swells arriving from remote sources. In the study described here, we have partitioned directional wave spectra derived from bottom-mounted ADCP measurements acquired south of Martha's Vineyard, MA, into dominant swell and locally generated wind-wave components. The partitioning was carried out following the method of Hanson and Phillips (2001). Because this is a relatively untested method, especially when applied to ADCP data, it was implemented by an exploratory, rather than a routine, approach. As part of this approach, we assessed the validity of the ADCP-derived wave spectra by comparing them with one-dimensional wave spectra derived from laser altimeter measurements. As will be shown, this comparison identified a frequency range over which the ADCP-derived wave field may be suspect. We also carried out sensitivity tests in which we evaluated how the results of wave partitioning according to the Hanson and Phillips (2001) method is influenced by varying the parameters required to implement the method. In the sections to come, we describe and assess the data sources used in our study, outline the methods employed for wave spectra partitioning and describe partitioning results (focusing on the sensitivity of these results to the partitioning parameters).

2. Data Sources and Processing

Carrying out the wave partitioning by the method of Hanson and Philips (2001) requires time series of directional wave height spectra and of wind velocity from the region where the spectra were acquired. For our study, these time series were derived using data from the Martha's Vineyard Coastal Observatory (MVCO). Sited off the southern coastal of Martha's Vineyard (Figure 1), the MVCO contains a suite of instrumentation acquiring continuous atmospheric and oceanic measurements, many of which are available in real time via an Ethernet network (see Edson et al., 2000, and Austin et al., 2002, for descriptions of the MVCO).

The analysis period, 30 July to 31 December 2003, was chosen to coincide with the 2003 Intensive Observing Period of the Coupled Boundary Layers/Air-Sea Transfer (CBLAST) research initiative (the low-wind component of CBLAST is described at <http://www.whoi.edu/science/AOPE/dept/CBLAST/low/cblastlow>). Below we briefly describe the instrumentation and processing methods used to generate the wind velocity and wave height spectra used in our study.

a. Wind Velocity

The MVCO includes a shore-based and a sea-based meteorological station (Figure 1; Table 1). The shore-based station, the MVCO meteorological mast, is located roughly 60 m from the mean low water mark and is equipped with a sonic anemometer at 10 m above mean sea level. The sea-based station, known as the Air-Sea Interaction Tower (ASIT), is located roughly 3 km south of Martha's Vineyard in approximately 15 m of water. The tower extends 23 m

above mean sea level. During the analysis period, the ASIT supported 5 sonic anemometers at heights of 5, 7, 11, 18 and 20 m above mean sea level. The ASIT wind record used for the partitioning analysis is a synthesized 10-m wind velocity record, computed by J. Edson using the available ASIT data from all levels. The winds were averaged to 20 min intervals matching the ADCP spectral processing intervals.

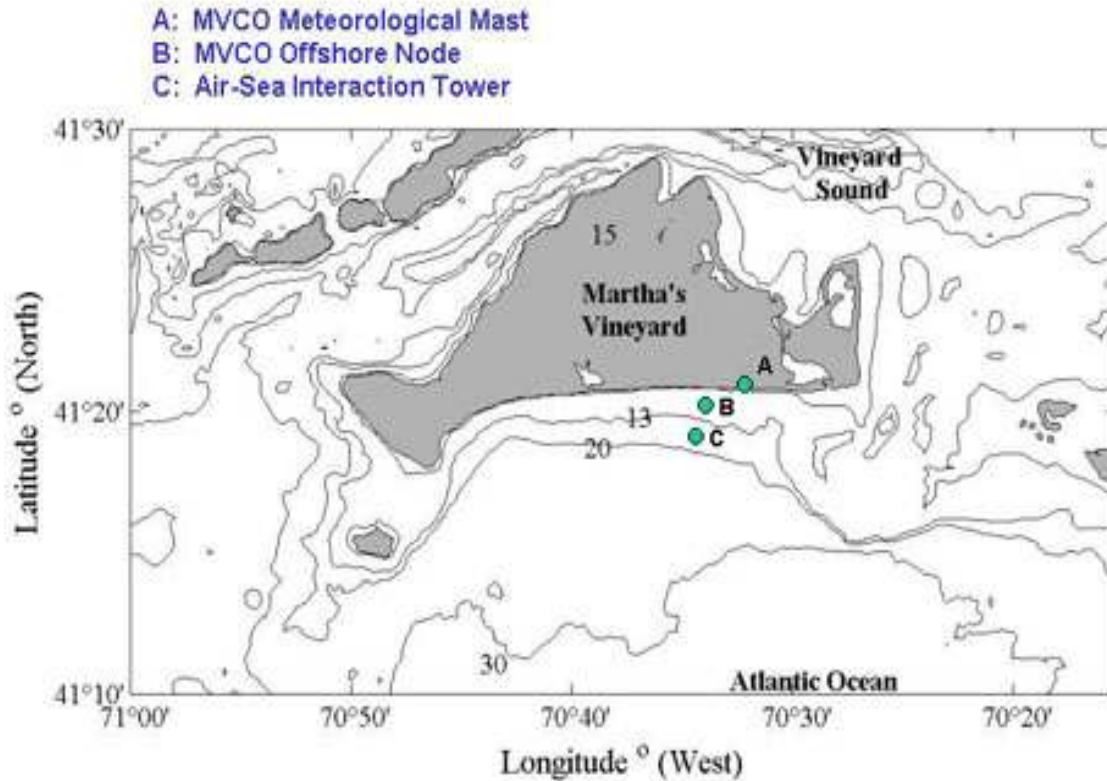


Figure 1. Locations of data used in this study. Wind velocity data were acquired at the Air-Sea Interaction Tower (C), and the MVCO meteorological mast (A). ADCP data used to compute wave directional spectra were acquired at the MVCO 12-m offshore node (B). One-dimensional wave spectra were derived from the measurements of a Riegl laser altimeter mounted on the Air_Sea Interaction Tower (C).

Unfortunately, the wind records for both stations contain long gaps, and neither fully encompasses the analysis period. Because the ASIT wind measurements are directly over the sea, they are deemed more appropriate for use in the wave partitioning analysis as they represent the “local” wind forcing of the wave field. Accordingly, wind velocities from the MVCO meteorological mast are employed only for those periods when ASIT winds are not available.

Fortunately, the winds from the two stations are closely matched at most times. For the 44-day wind records shown here (Figure 2), the magnitudes of the vector differences between the ASIT and MVCO shore-based wind velocities have an average of 1 m s^{-1} and a standard

deviation of 0.6 m s^{-1} . When plotted against one another, the vector components of the ASIT and MVCO shore-based winds are tightly clustered about the one-to-one match lines (Figure 3).

Table 1. Locations of measurements used in our study.

Instrument	Latitude	Longitude	Description
MVCO meteorological mast	41° 20.996' N	70° 31.60' W	Shore-based tower with a sonic anemometer at 10-m
ASIT	41° 19.500' N	70° 34.0' W	Sea-based tower supporting 5 sonic anemometers
ADCP	41° 20.195' N	70° 33.387' W	1200-kHz RD Instruments Workhorse ADCP Wave gauge deployed at the MVCO 12-m depth node
Laser Altimeter	41° 19.500' N	70° 34.0' W	Riegl Altimeter mounted on the ASIT tower

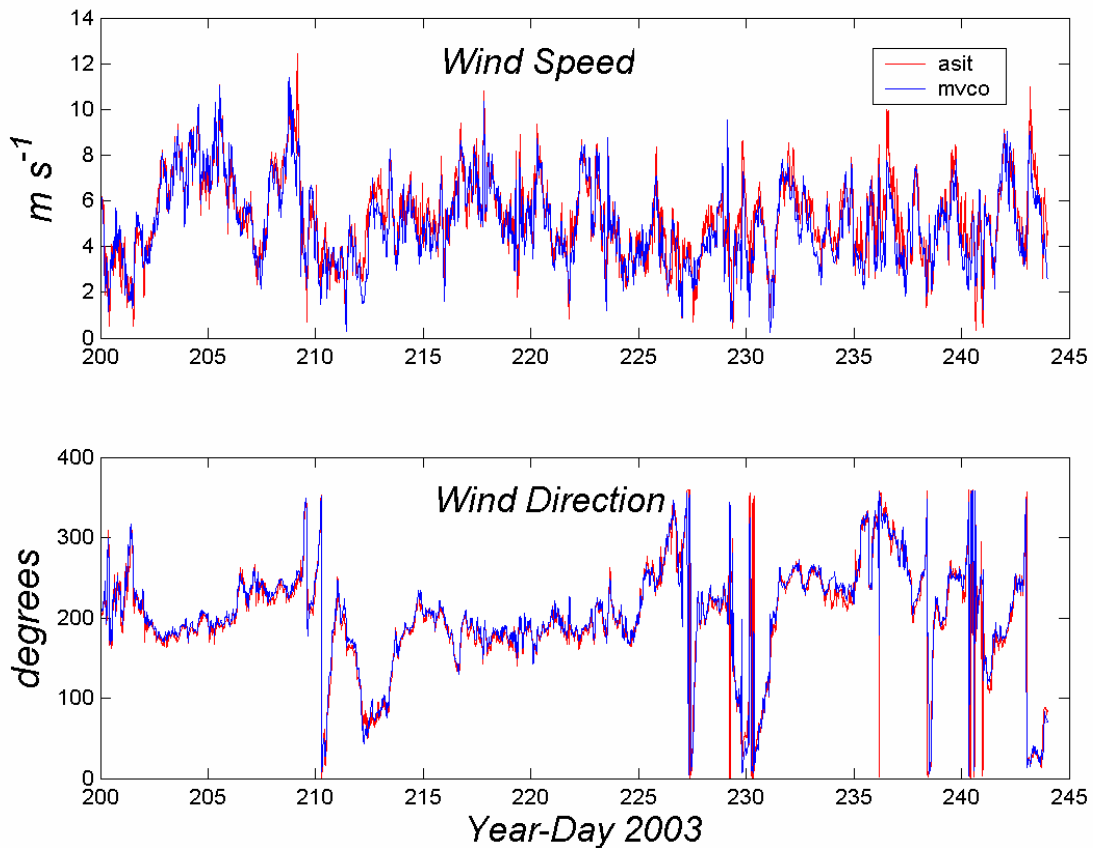


Figure 2. Comparison of 10-m wind records from the ASIT offshore tower (red) and the MVCO shore mast (blue) (see Figure 1 for locations). Wind directions are in “meteorological convention,” so that 180° means a wind from the south.

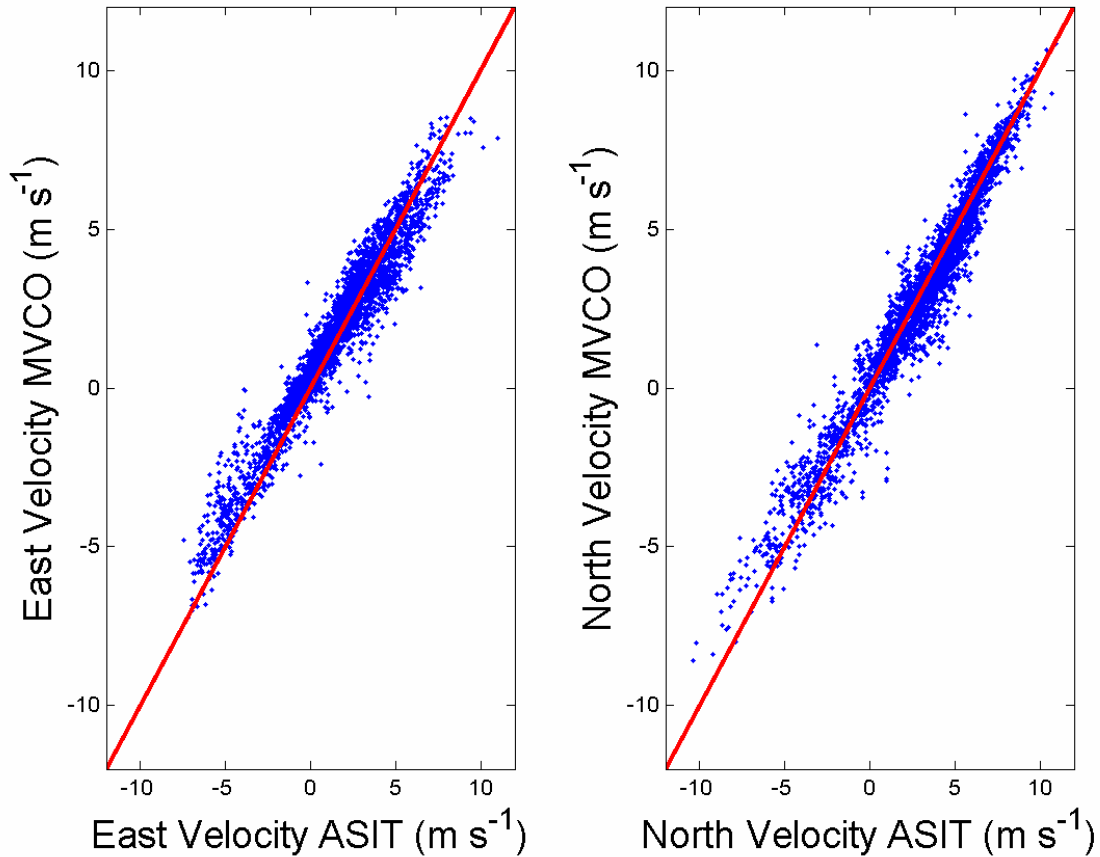


Figure 3. Comparison of the velocities measured at the ASIT offshore tower and the MVCO shore mast. As in Figure 2, the values shown are from year days 200-244 of 2003. The red line in each panel traces a one-to-one match in the velocity component.

b. Laser Altimeter-Derived Wave Spectra

The laser altimeter measurements of sea surface height used in our study are from a Riegl altimeter deployed on the ASIT tower (Figure 1, Table 1) and were provided courtesy of J. Edson. The altimeter sampled at a frequency of 20.4 Hz.

In computing sea surface height spectra from the altimeter measurements, we first divided the altimeter height time series into 20-minute segments. A spectrum of each segment was computed by averaging spectra from overlapping sub-segments of length 8192 points. A Hamming filter was applied to each sub-segment prior to spectral computation via a fast Fourier transform. The resulting time series of spectra, with a frequency resolution of .0025 Hz and a time interval of 20 minutes, was smoothed by applying a 3-point running mean filter over both time and frequency.

This time series of sea surface height spectra is not continuous, as the laser data set contains frequent gaps, many of which extend for > 1 d. Nevertheless, the height spectra have

proven useful in assessing the wave spectra derived from the ADCP velocity data, as described below.

c. ADCP-Derived Wave Spectra

The directional wave spectra used in the wave partitioning analysis were computed from velocity data acquired from an upward-looking ADCP deployed at the MVCO 12-m node (Figure 1, Table 1). Supported by a pedestal base jettied 12 ft into the sea bed, the node is located roughly 1.5 km from shore in 12 m of water. The ADCP acquired data at 2 Hz and determined velocities in bins of 0.5-m thickness. The deepest bin is 3.2 m above the bottom.

Directional wave spectra were computed from the ADCP velocity data using the Teledyne RD Instruments WavesMon software package. The principals of operation of this software package are described in the RDI Waves Primer (available at: http://www.rdinstruments.com/pdfs/waves_primer_0504.pdf) and by Krogstad et al. (1988), Terray et al. (1999) and Strong et al. (2000). In the most basic terms, WavesMon operates by assuming that the auto- and cross-spectra of the velocity series determined from the returns of the individual acoustic beams are related, through known linear functions, to the directional wave distribution. An iterative maximum likelihood method is employed to determine the directional wave field in best agreement with the ADCP velocity auto- and cross-spectra.

For our study, directional wave spectra were determined using WavesMon from successive 20-min segments of the ADCP data. These spectra, each with a resolution of 0.0078 Hz and 4°, were filtered in frequency and direction with a 3x3 median filter and further smoothed in frequency with a 3-point running mean filter. These operations produced a continuous time series of wave directional spectra, at 20-min intervals, extending over year-days 211-365 of 2003 (30 July–31 December in our year-day convention in which noon on 1 January is year-day 1.5).

d. Comparison of ADCP- and Laser Altimeter-Derived Wave Spectra

Wave properties determined from ADCP data via WavesMon have been evaluated by at least two teams of investigators. Rørbaek and Anderson (2000) compared ADCP-derived wave properties with those determined using data from an Inter Ocean S4 bottom-mounted electromagnetic current meter. They found wave statistics (*e.g.*, significant wave height, wave peak period) derived from the S4 and ADCP data to be in close agreement (generally differing by less than 5%). Strong et al. (2000) compared wave properties determined from ADCP data acquired at a number of locations with data obtained from other instruments, principally an Acoustic Doppler Velocimeter (ADV) and a WaveRider buoy. They also reported close agreement between the ADCP-derived wave statistics and those determined from the independent measurements.

Although these studies provide confidence in the wave spectra determined by WavesMon, the relative youth of the WavesMon application makes it worthwhile to compare WavesMon generated wave spectra with wave spectra derived from independent measurements whenever possible. For such a comparison, the laser altimeter data are in many respects ideal, since they are direct measurements of surface waves and encompass very high frequencies. Subsurface measurements of wave motions, such as the ADV data used in the comparison by Strong et al.

(2000), are limited by a high frequency cutoff in wave detection due to the rapid attenuation of high frequency surface waves with depth.

To compare the ADCP-derived wave spectra with the wave spectra computed from the laser altimeter measurements, the two-dimensional ADCP-derived spectra were integrated over direction. The resulting 1-dimensional spectra compared well with the spectra derived from the laser altimeter measurements in the period band that typically contains most of the surface wave energy (2.4-12 s) (Figures 4 and 5). At most times, the peaks in the spectra derived from the laser altimeter data were higher and sharper than the corresponding peaks observed in the spectra determined from the ADCP data (Figure 5). Both the lower frequency resolution and the additional frequency smoothing of the ADCP spectra contribute to this difference.

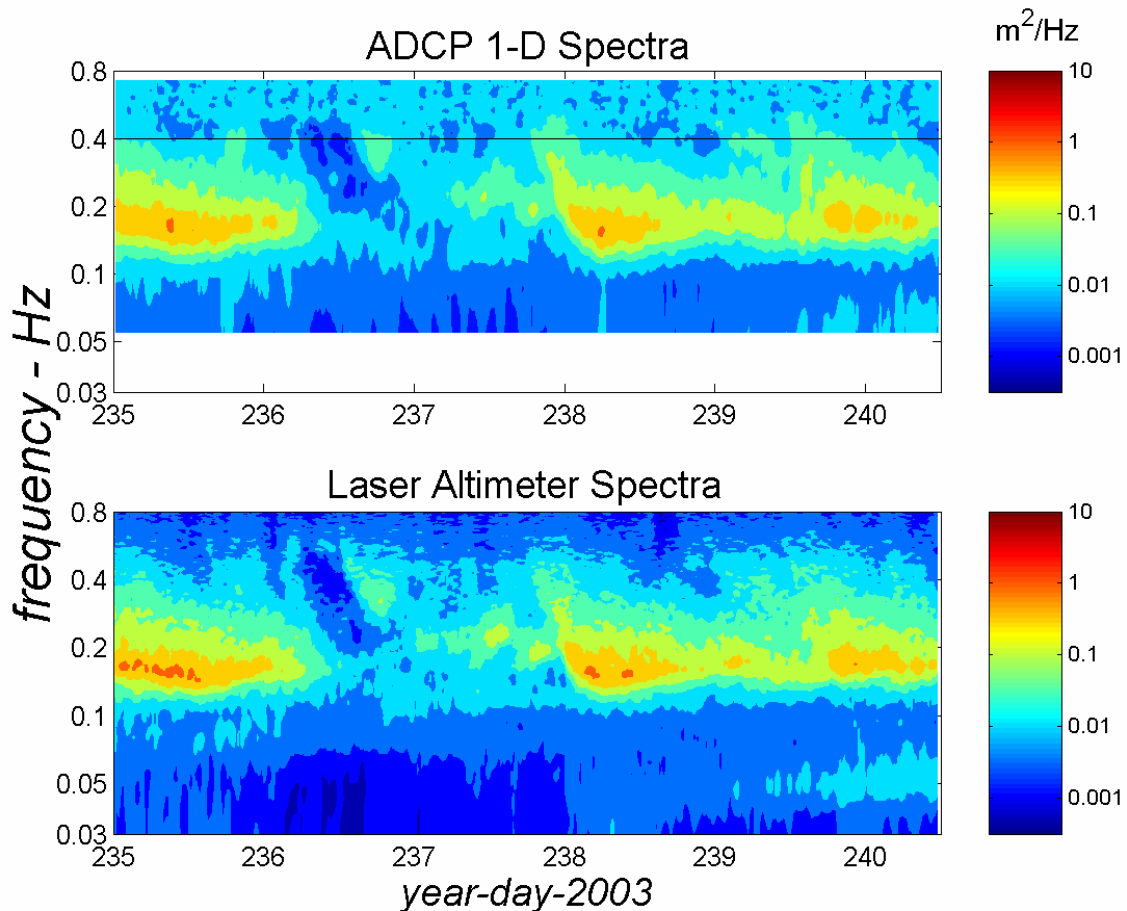


Figure 4. Comparison of 1-dimensional wave spectra derived from ADCP data (top panel) and laser altimeter measurements (bottom panel). The horizontal line in the upper panel marks the high frequency cutoff (at 0.4 Hz) for the spectra passed to the wave partitioning routine.

At frequencies above 0.4 Hz, the wave spectral estimates derived from the ADCP data are consistently higher, by roughly a factor of two, than those determined from the altimeter data. Close comparison of the high frequency ADCP- and altimeter-derived wave estimates reveal differences between the two that cast doubt on the validity of the high frequency ADCP-derived estimates. At frequencies > 0.4 Hz, the laser altimeter-derived spectral magnitudes tend to

decline with frequency whereas the ADCP spectral estimates are essentially flat (Figure 5). In this higher frequency band, the ADCP-derived energy levels exhibit temporal modulations, at periods of < 1 d, that are not apparent in the altimeter derived spectra (Figure 4). These differences between the ADCP-derived spectra and the presumably reliable laser altimeter-derived spectra make the high frequency ADCP-derived wave spectral estimates highly suspect. For this reason, we truncated the ADCP spectra at a high frequency cutoff of 0.4 Hz, before these spectra were used as input to the wave partitioning software.

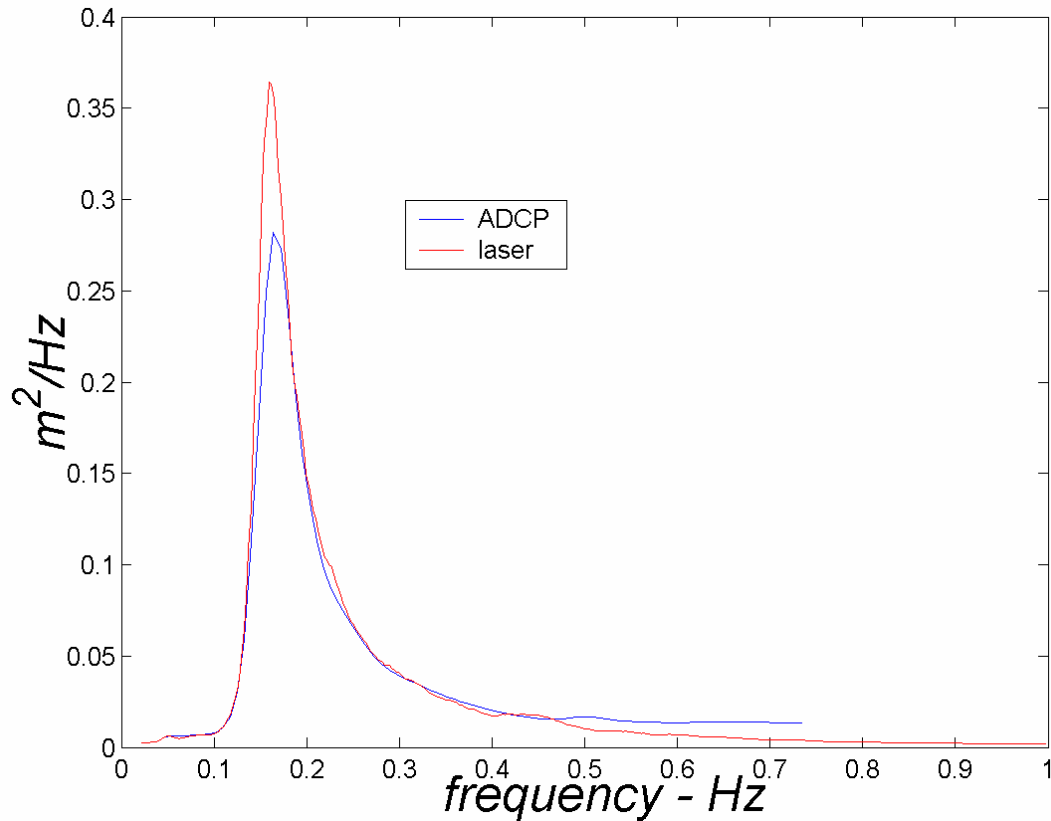


Figure 5. Time averages of the ADCP and laser altimeter-derived spectra shown in Fig. 4. The altimeter spectral peak is about 30% higher and also narrower than that of the ADCP. This is due in part to the lower frequency resolution and increased frequency smoothing of the ADCP spectra.

3. Wave Spectra Partitioning

a. Wind Sea Identification

Our partitioning of the ADCP-derived directional wave spectra was carried out using the software routine APL-WAVES (<http://www.subchem.com/waves>), which employs the methodology described by Hanson and Phillips (2001). A commercially sold software product developed in MATLAB (<http://www.mathworks.com>) Version 6.5, APL-WAVES is designed to identify portions of a directional wave spectra that are due to the locally generated “wind sea” and to swells from distant sources. The program determines the presence, or absence, of a wind

sea by imposing an “age criterion” such that the phase speed (c_p) of the wind-sea spectral peak (or peaks) satisfies the relationship

$$c_p \leq W_M U_{10} \cos \delta$$

where U_{10} is the wind speed at 10 m, δ is the angle between the wind and wind sea, and W_M is a “wind-sea multiplier.” By applying the deep water wave dispersion relationship, the above defines a parabolic region of the directional wave spectrum within which the wind-sea peak is required to reside (Figures 6 and 7). This region is defined by

$$f_p \geq \frac{g}{2\pi} [W_M U_{10} \cos \delta]^{-1}$$

where f_p is the spectral peak of the wind sea and g is the gravitational acceleration. All other spectral peaks are assumed to be produced by swell. These swell peaks are separated, or combined, based on the degree of peak separation and the energy level between peaks.

The conventional limit of applicability for the deep water dispersion relation (~10% error in the dispersion relation) is $H = L / 4$, where H is the water depth and L is the wavelength. In 12 m water depth this limit gives a maximum wavelength of 48 m, corresponding to a maximum wave period of about 5.8 s. More than 90% of the wind seas identified by APL-WAVES (Section 4b) have periods less than this limit, indicating that the use of a wind-sea parabola based on deep-water dispersion will not significantly affect the results. Furthermore, inspection of the APL-WAVES output shows that some fraction of the long-period wind waves ($T > 7$ s) are in fact mis-identified swell (due to short-term increases in U_{10} that increase f_p in the absence of significant wind-wave growth). Still, some problems could arise in identifying the rare cases of actual long-period wind waves, since the deep-water f_p will be too high by the factor $\tanh(kh)$, which approaches 20% for $T = 7$ s. However, the relatively generous values of the wind-sea multiplier used in this study ($1.4 \leq W_M \leq 1.9$) tend to mitigate such problems.

b. APL-WAVES Parameters

The program defines a set of parameters to identify the wind sea and distinguish swell spectral peaks. The user may employ default values or adjust the parameters to suit his/her requirements. The parameters control the program’s function in four broad categories. These parameters are listed and described below together with their default values (in square brackets) for ADCP-derived spectra.

Wave Height Thresholds: These parameters are set to minimize the possibility of identifying spurious, low-energy peaks in the directional wave spectrum as either a developing wind sea or a swell from a distinct source.

- Minimum Wind-Sea Height [0.1 m]
- Minimum Swell Height [0.2 m]

Wind Sea Selection: As described above, the multiplier is used to define the parabolic area within which a spectral peak is considered part of the wind sea.

- Wind-Sea Multiplier, W_M [1.9]

Swell Selection: The first parameter defines the maximum number of swell “systems” allowed per spectra. The swell systems are sorted based on total energy. The second and third parameters are used to determine if spectral peaks belong to the same, or different, swell systems. Adjacent peaks are combined if they are less than the Spread Factor times the “spread of either partition.” Adjacent wave spectral peaks are assigned to different swell systems if they differ in direction by more than the Swell Separation Angle.

- Number of Swells Per Record [3]
- Spread Factor [1]
- Swell Separation Angle [40°]

Wave System Tracking: Wave tracking parameters control the manner in which APL-WAVES links wave systems through time. The first parameter defines the maximum number of consecutive records that may be missing while still attempting to link the wave systems. The second parameter specifies the minimum number of consecutive records for a valid swell system to be identified.

- Largest Record Gap [4]
- Minimum Number of Records [10 m]

Evaluating the effect of these parameters on the operation of APL-WAVES was facilitated by the spectral plots generated by the program that distinguish the different wave systems identified by the partitioning. To demonstrate the utility of these plots, we offer here two examples of spectra partitioned using the “default” parameters. In one, the spectral peaks are broadly separated, and use of the default parameters clearly distinguishes the wind sea and a dominant swell system (Figure 6). By contrast, the other spectrum has more closely spaced peaks that clearly offer more of a challenge to the partitioning routines (Figure 7). In the next section we describe our attempt to hone the parameters for optimal partitioning of the MVCO directional wave spectra.

4. Results

a. Parameter Sensitivity Tests

In an attempt to optimize the operation of APL-WAVES, we carried out a series of sensitivity tests, exploring how variation of key parameters affects the manner in which the program identifies the wind sea and remotely generated swell systems. The goal was to select a parameter set that produced optimal results with regard to wind sea and swell system identification. In carrying out the sensitivity tests, we held certain parameters, deemed least

critical, constant at their default values (Section 3b). These were: the number of swells per record, the largest record gap and the minimum number of records.

In exploring the effect of the other parameters, we focused on four periods, 2003 year days: 228-232.5 (August 16-20), 240-243 (August 28-31), 280-283 (October 7-10) and 291-294 (October 18-21). These periods encompassed a wide variety of wind and wave conditions. Here we present and discuss the sensitivity tests from year day 240-243 only. The spectra of this period exhibited a sufficient range of differing wave conditions from which to judge different aspects of the partitioning routines.

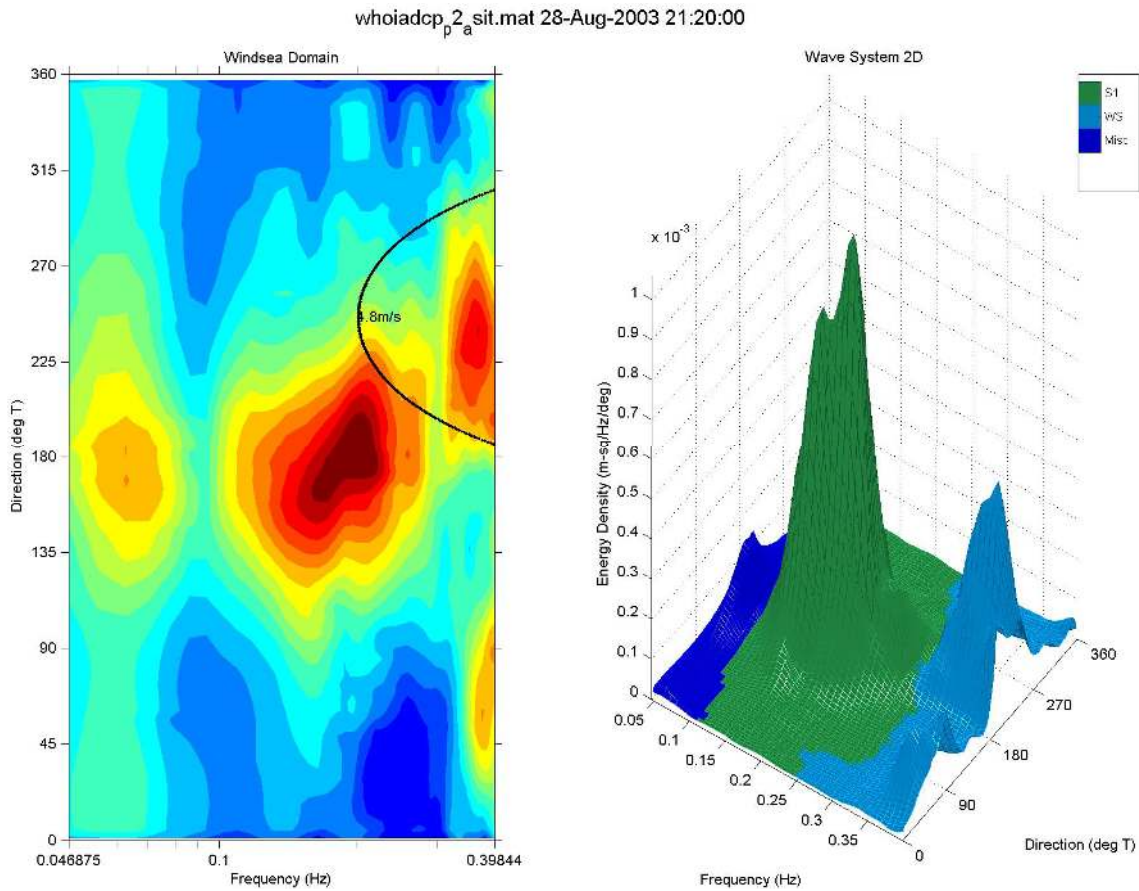


Figure 6. An example of an ADCP directional wave spectrum partitioned using the default parameters of APL-WAVES. The plot on the left shows the contoured spectrum with the wind-sea parabola superimposed. The plot to the right shows the spectral regions APL-WAVES identified as the wind sea (light blue), dominant swell (green) and miscellaneous (dark blue). The plots were generated by APL-WAVES.

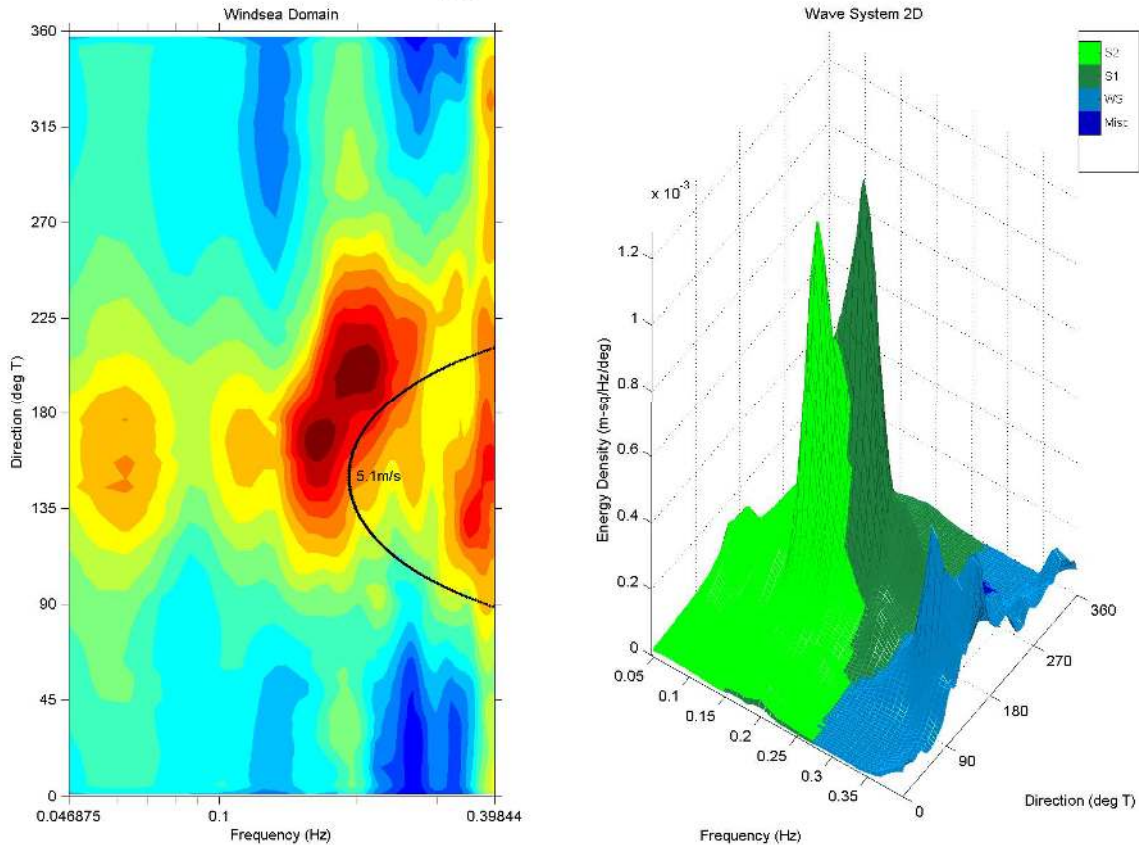


Figure 7. Same as Figure 6 except showing the partitioning results of a somewhat more complicated spectrum. Note that the program separated the closely spaced wave peaks at roughly 0.2 Hz into two swell systems, but also lumped a well separated, lower frequency peak (near 0.07 Hz) into one of these systems (identified by the light green coloring in the right hand plot).

Selection of the “optimal” parameter set was largely a subjective process, and involved balancing the positive and negative effects of varying a certain parameter. Assessments were formed from examining the wave partition plots generated by APL-WAVES and by tracking the continuity of wave properties (such as averaged wind sea and swell system frequency) over time. In all, we compared the results from nine parameter sets (Table 2) which are presented in Figures 8-16.

The two parameters that control the identification of the wind sea are the minimum wind-sea height and the wind-sea multiplier. The former limits the identification of spurious high frequency motions as a wind sea. However, too small a value of minimum wind-sea height may preclude the detection of a wind sea during its early development. Through examination of sequences of wave spectra from times of a newly developing wind sea, we found that a threshold of 0.075 m allowed APL-WAVES to successfully capture the nascent wind sea with very few false identifications of spurious motions as wind sea.

Table 2. Parameter sets used in the partitioning sensitivity tests.

Designation Letter	Min. Wind Sea Height	Min. Swell Height	Wind Sea Mult.	Spread Factor	Swell Separation Angle
<i>a</i> (default)	0.1 m	0.2 m	1.9	1	40°
<i>b</i>	0.075 m	0.2 m	1.6	1	40°
<i>c</i>	0.075 m	0.1 m	1.6	1	40°
<i>d</i>	0.075 m	0.1 m	1.4	1	40°
<i>e</i>	0.075 m	0.1 m	1.8	1	40°
<i>f</i>	0.075 m	0.1 m	1.6	0.4	40°
<i>g</i>	0.075 m	0.1 m	1.6	0.7	40°
<i>h</i>	0.075 m	0.1 m	1.6	0.7	20°
<i>i</i>	0.075 m	0.1 m	1.6	0.4	20°

The principal concern governing the selection of the wind-sea multiplier is to capture the spectral peak of a developing sea in the wind-sea parabola while excluding spectra peaks due to swell from the parabola. Too small a multiplier may put spectral peaks clearly associated with a wave sea outside the reach of the parabola. However, too large a multiplier may overextend the parabola to capture spectral peaks due to remote swell. The assessment of the wind-sea multiplier is further complicated by situations in which wind speed and/or direction vary dramatically during the generation of a wind sea. A short-term dip in wind speed, for example, can produce a scenario in which a spectral peak due to a developing wind sea is temporally outside the scope of the wind-sea parabola.

We tested the program’s operation with wind-sea parameters in the range of 1.4 to 1.9 (the program’s default value for ADCP-derived spectra). Values of 1.8 and 1.9 appeared to be too large as they often extended the wind-sea parabola to include the spectral peaks clearly associated with swell (Figure 17).

The partitioning of the spectra from year days 140-141.5 offer a number of instances of this sort of wind-sea parabola overextension. The spectra from this period contain a high frequency swell system with peak energy at roughly 0.18 Hz. Using wind-sea multipliers of 1.8 and 1.9 often results in the inclusion of this swell system into the wind-sea domain (Figures 8 and 12). The frequency of this overextension of the wind domain is significantly lessened by reducing the multiplier to 1.6 (Figure 10) and is virtually eliminated by a further reduction of the multiplier to 1.4 (Figure 11). However, use of a 1.4 multiplier is seen to be problematic for the capture of a low level wind sea appearing near 0.42 Hz in the spectra from the year day range 241-241.5. The spectral peak of this wind sea is often outside the domain of the wind sea defined with a 1.4 multiplier (Figure 11), but is much more often within the wind-sea domain defined with a 1.6 multiplier (Figure 10). Examination of the partitioning results from the other periods listed above revealed similar tendencies for an overextension of the wind-sea parabola at multipliers ≥ 1.8 and an occasional exclusion of a wind-sea peak from the wind-sea domain determined with a multiplier of 1.4. For this reason, we chose 1.6 as the “compromise” wind-sea multiplier that best captured the wind sea under most conditions.

The principal parameters controlling the detection and separation of swell systems are the minimum swell height, the spread factor and the swell separation angle. We found that running APL-WAVES with the default minimum swell height of 0.2 m often relegated distinct, but low energy, spectral peaks to the “miscellaneous” category. Reducing the minimum swell height to 0.1 m resulted in the designation of many more of these low energy spectral peaks as swell systems.

For most spectra, we found that partitioning with the default parameters for spread factor (1) and swell separation angle (40°) separated clearly distinct low frequency peaks into different swell systems. However, there were a number of spectra with distinct and closely aligned peaks that were lumped into a single swell system with the use of the default parameters (Figure 18). These spectra were usually from periods with relatively low wave energy. For many such spectra, reducing the spread factor to 0.7 resulted in the generation of one or more additional wave systems to accommodate the distinct spectral peaks (Figure 18, middle panel). Further reduction of the spread factor, however, often caused APL-WAVES to draw too sharp a distinction between wave systems, dividing what appeared to be a single spectral peak into separate wave systems (Figure 18, bottom panels). The reduction of the swell separation angle from the default value often had the same effect of dissecting an apparently single spectral peak. Based on these observations, we conclude that of spread factor/separation angle combinations tested, 0.7/ 40° produced the best swell system partitioning.

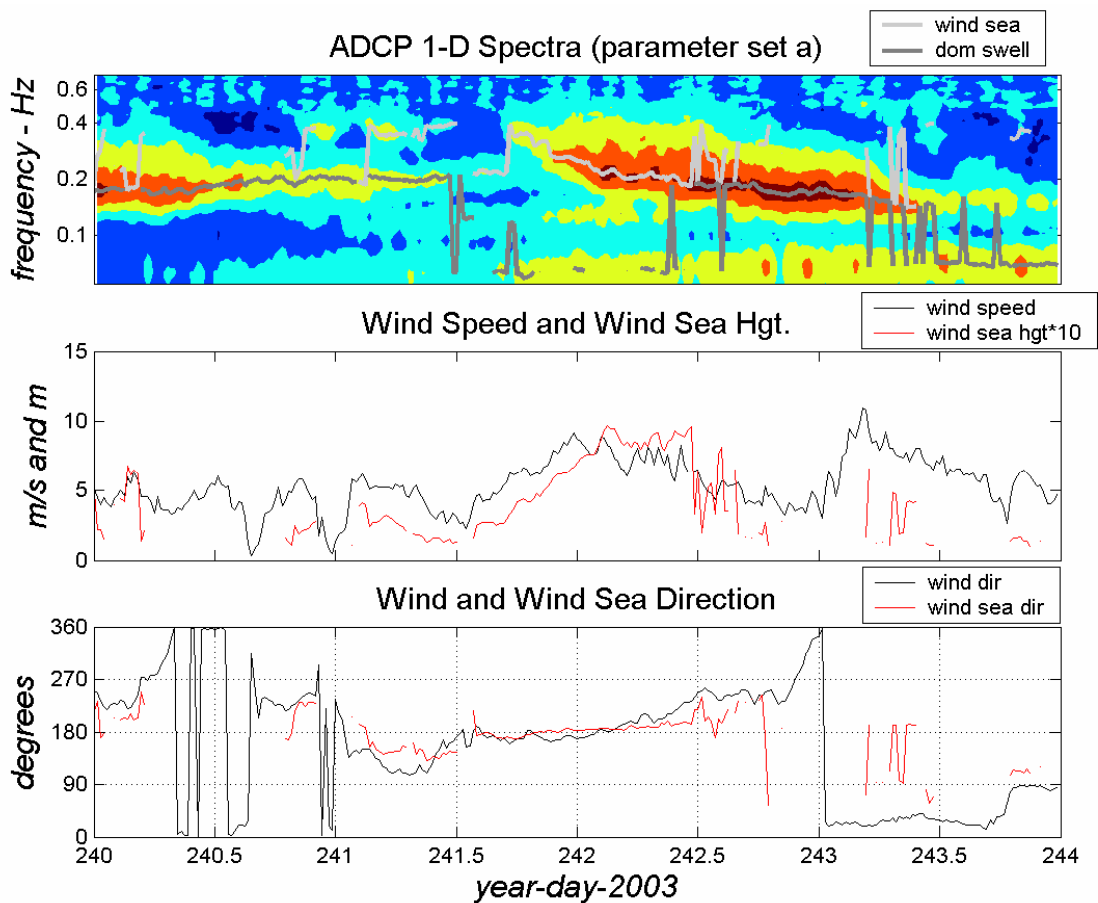


Figure 8. The top panel shows contoured wave energy, on a time-frequency plane, determined by integrating the ADCP-derived directional wave spectra over direction. Superimposed on the contours are lines tracing the characteristic frequency (energy-weighted average) of the wind sea and dominant swell. The middle panel shows the ASIT wind speed and wind-sea significant wave height. The bottom panel displays wind direction and energy-weighted mean wind-sea direction. All wave properties were determined using parameter set *a* (Table 2).

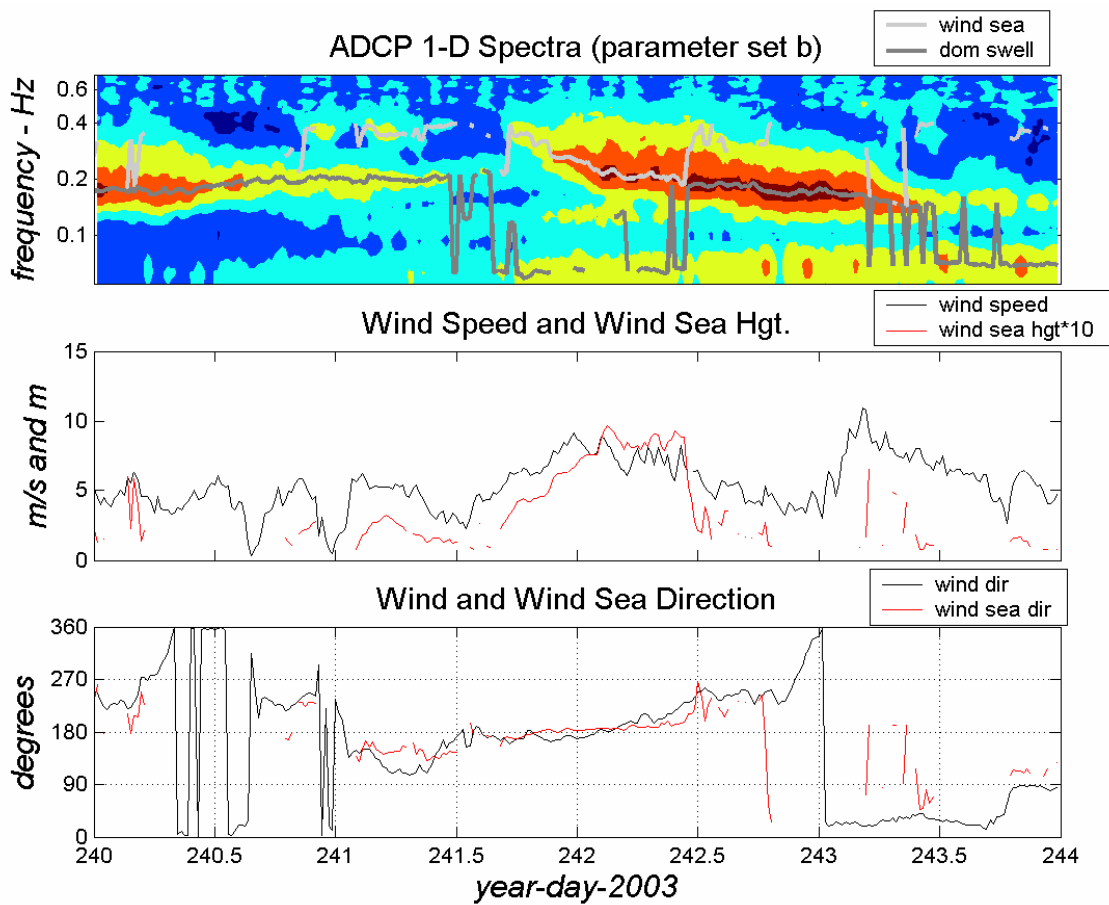


Figure 9. Same as Figure 8 except computed using parameter set *b* (Table 2).

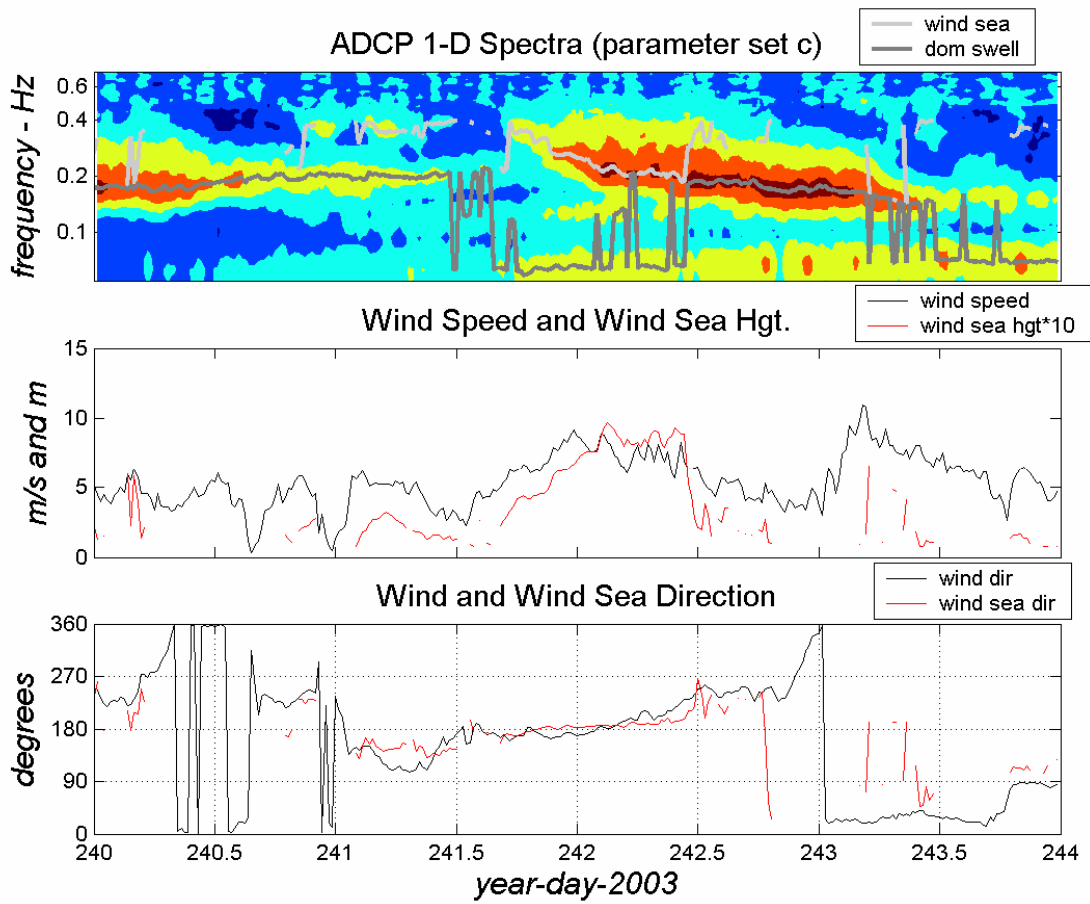


Figure 10. Same as Figure 8 except computed using parameter set *c* (Table 2).

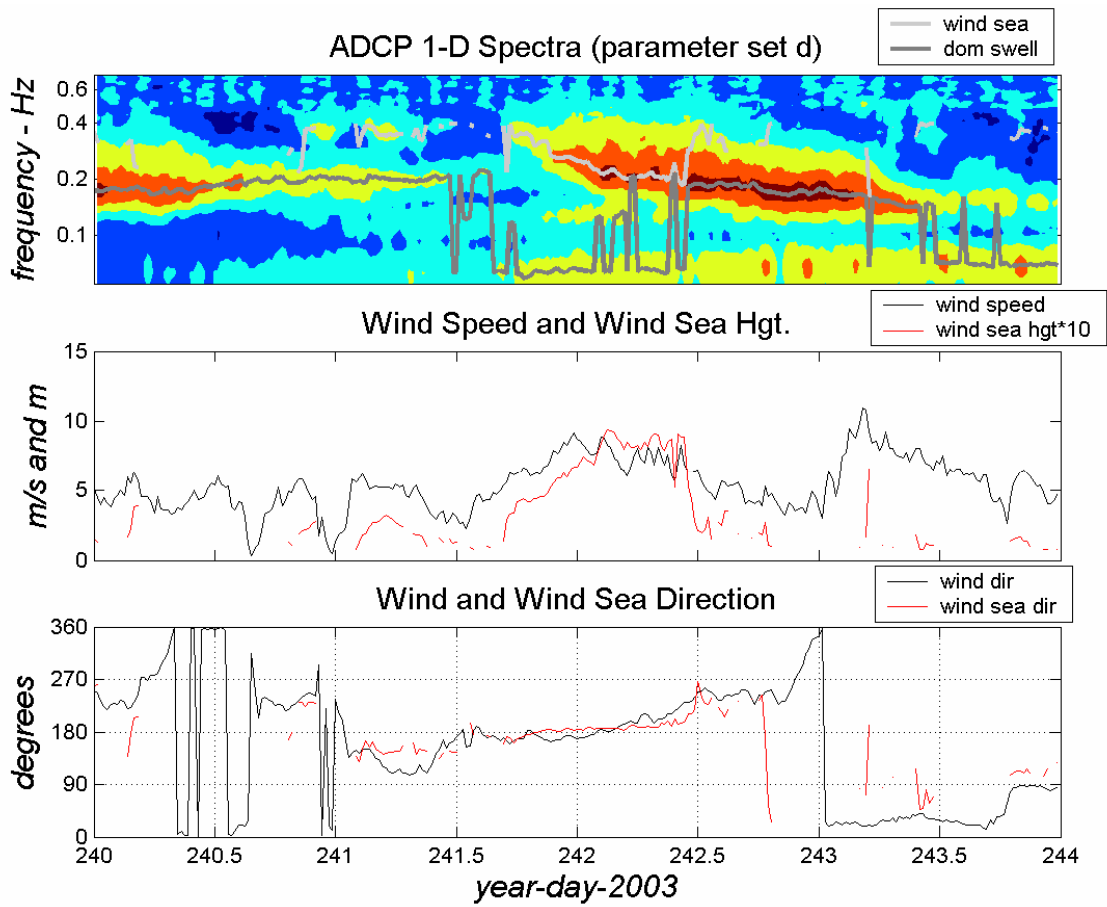


Figure 11. Same as Figure 8 except computed using parameter set *d* (Table 2).

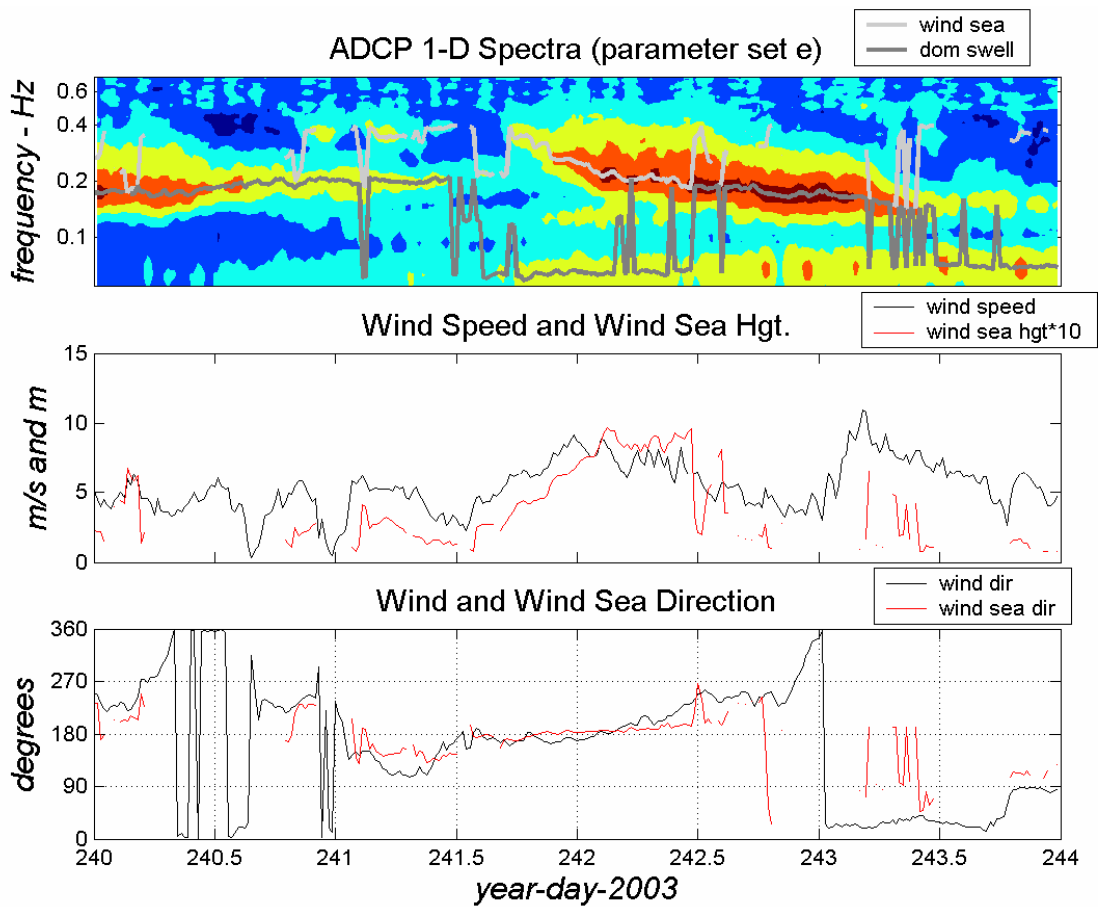


Figure 12. Same as Figure 8 except computed using parameter set *e* (Table 2).

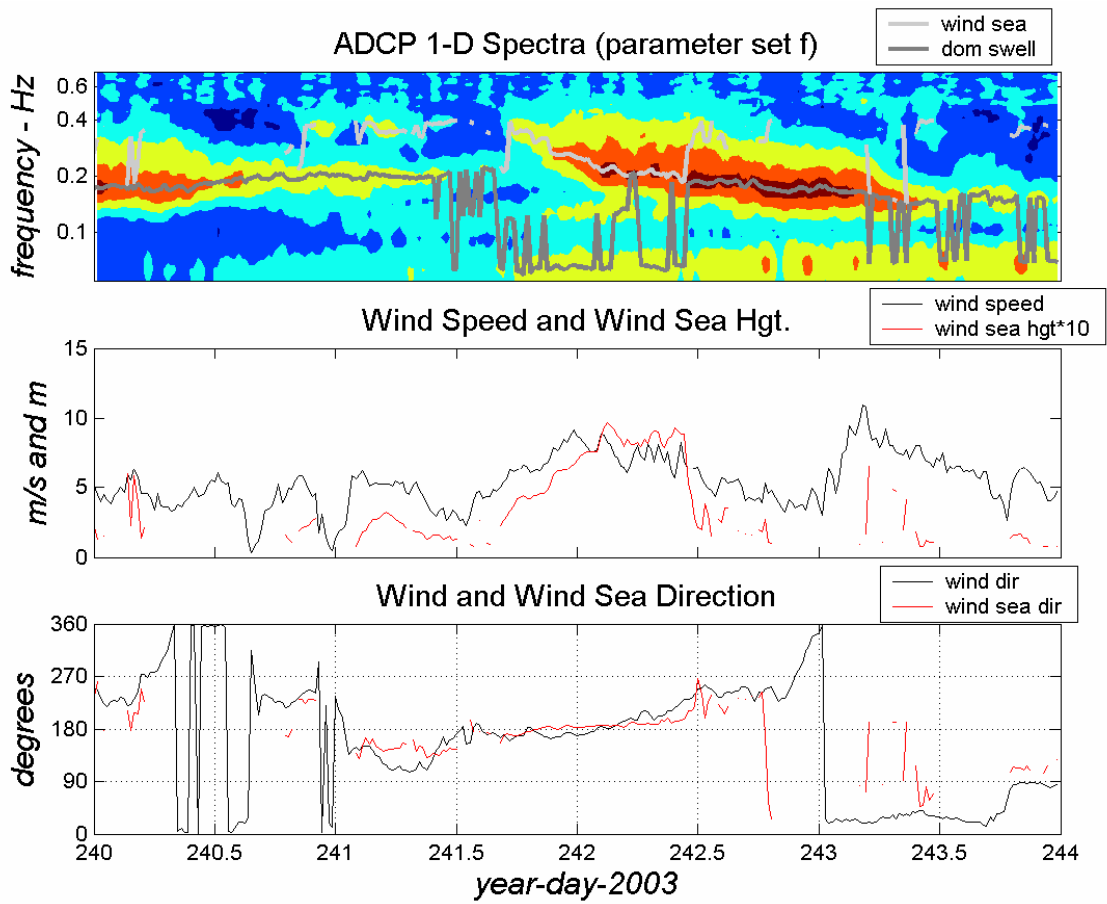


Figure 13. Same as Figure 8 except computed using parameter set *f* (Table 2).

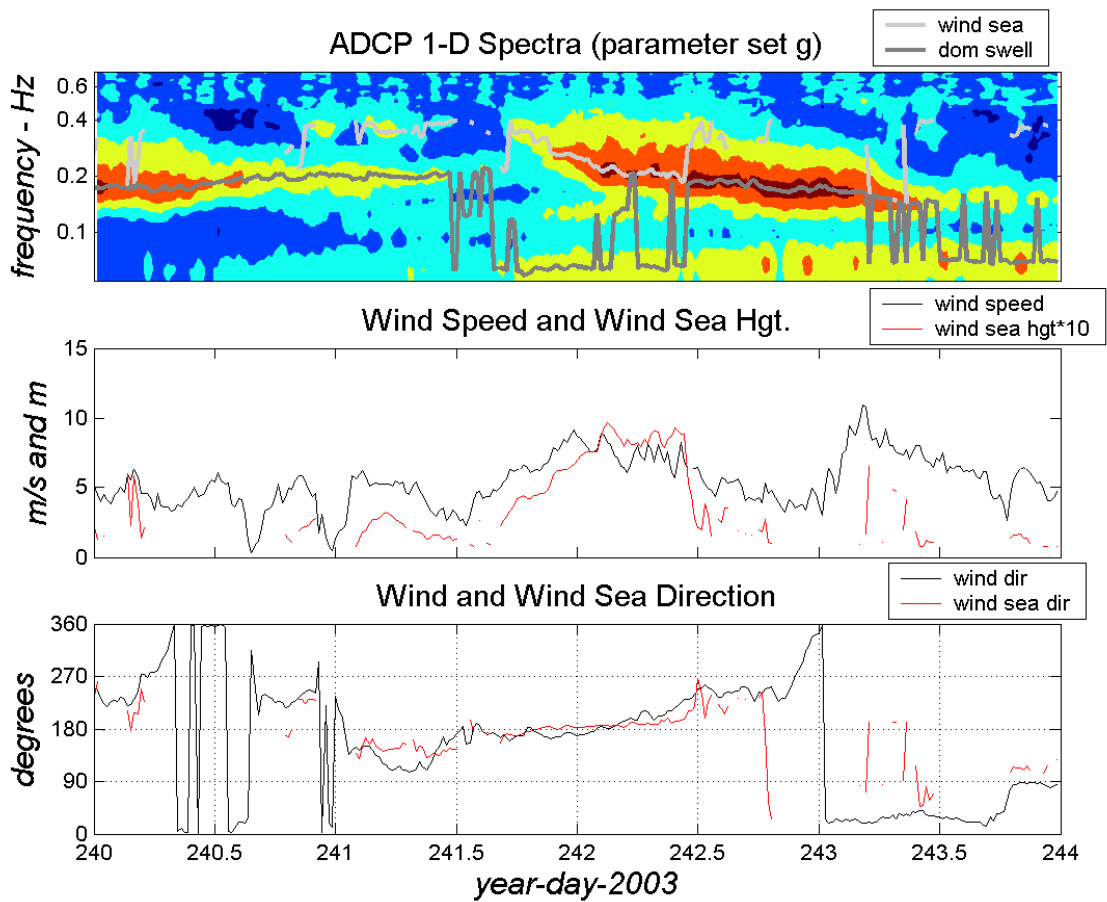


Figure 14. Same as Figure 8 except computed using parameter set g (Table 2).

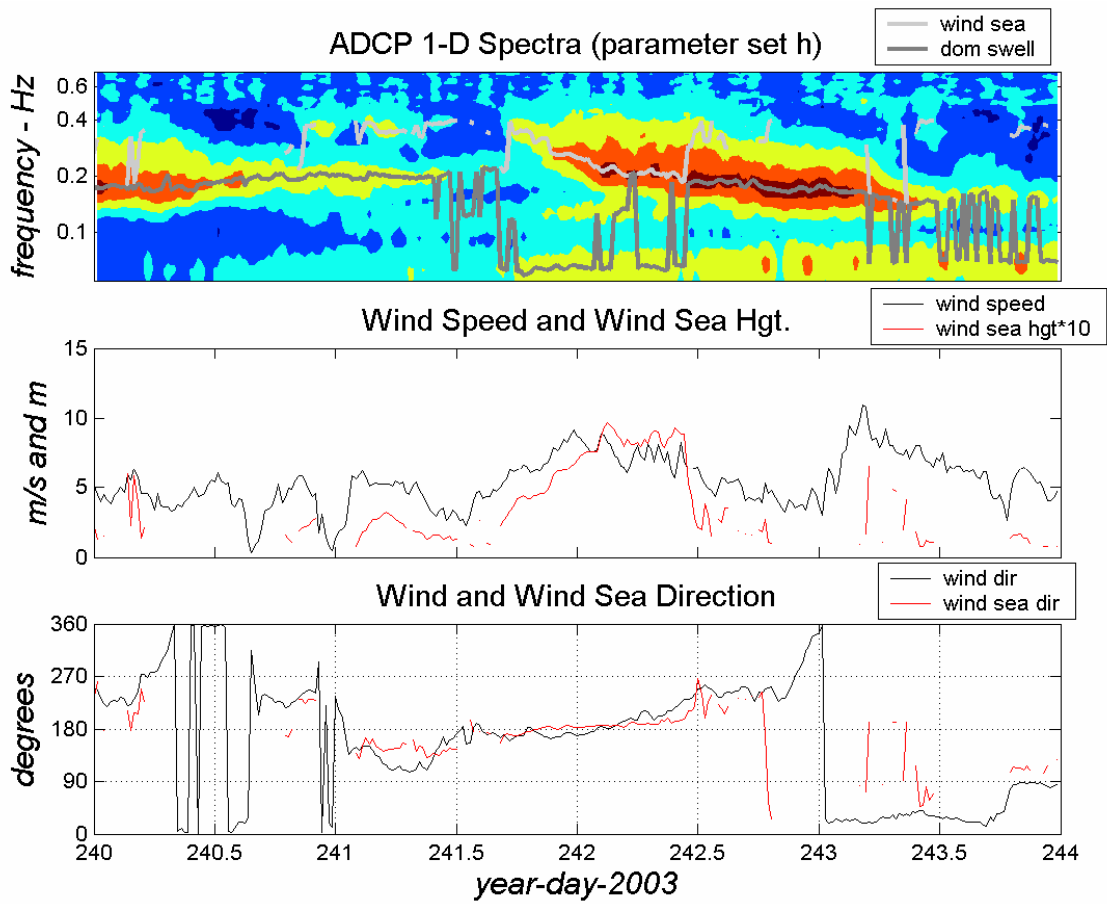


Figure 15. Same as Figure 8 except computed using parameter set *h* (Table 2).

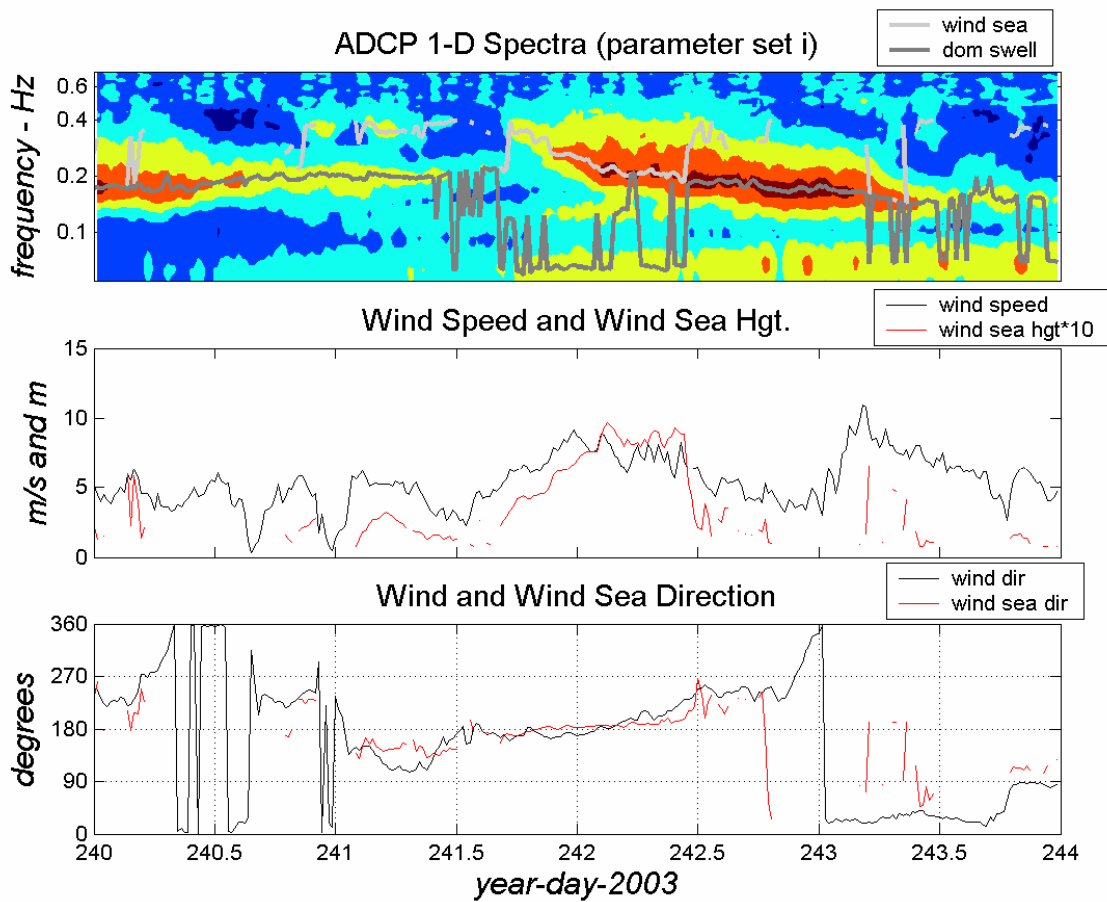


Figure 16. Same as Figure 8 except computed using parameter set *i* (Table 2).

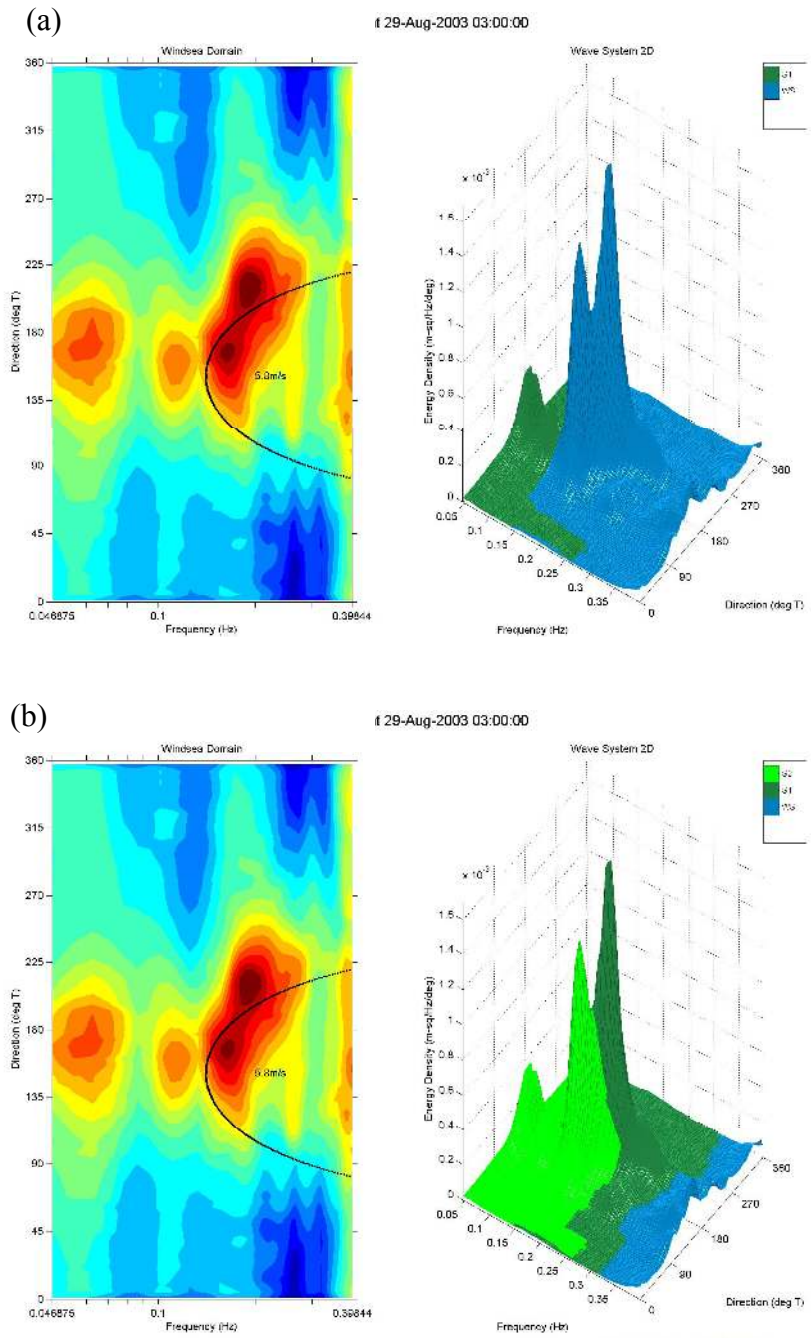


Figure 17. Comparison of the wind sea-portions of spectra determined with a wind-sea multiplier of 1.8 (top panels, parameter set *e*) and 1.6 (bottom panels, parameter set *c*). Partitioning with the larger wave multiplier causes spectral peaks associated with a swell system to be included in the wind-sea spectral domain.

August 29, 2003 10:00

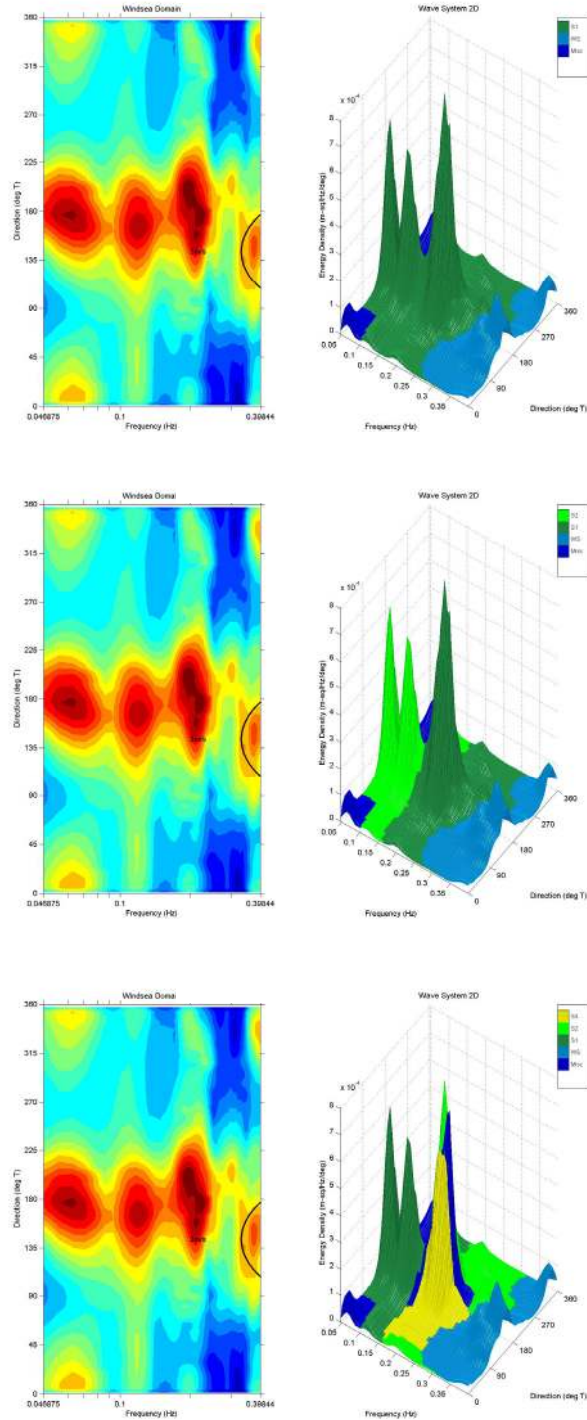


Figure 18. Comparison of a wind spectrum partitioned with three different combinations of spread factor and swell separation angle. Partitioning of the top, middle and bottom panels were carried out with spread factor/separation angle combinations of $1/40^\circ$ (parameter set *c*), $0.7/40^\circ$ (set *g*) and $0.4/20^\circ$ (set *i*), respectively. For this spectrum, the $0.7/40^\circ$ spread factor/separation angle combination produced a reasonably good separation of swell systems, whereas the $0.4/20^\circ$ combination appeared to divide swell systems too finely.

b. Output of Spectral Partitioning

To summarize the above, we found that of the parameter sets tested (Table 2), use of set *g* produced the best partitioning results. With this set as input to APL-WAVES, we partitioned all spectra derived from the MVCO ADCP for the period July 30–December 31, 2003 (year-days 211-365). From the program’s output, we generated a MATLAB binary file (*wave_statistics.mat*) with variables describing the statistical properties of the overall wave field, the wind sea, and the dominant and secondary swell systems. All variables were computed as defined in Hanson and Phillips (2001). A brief description of each variable is provided in Appendix 1. So that the statistical properties of the directional spectra could be easily compared with the frequency distribution of wave energy, we also generated a MATLAB file (*spec_1d.mat*) containing a time series of the one-dimensional wave energy spectra (determined from integrating the directional spectra over frequency) derived from the ADCP data for the period listed above. These data files, together with two routines (*contour_spec_1d.m* and *rmfltr.m*, written in MATLAB 6.5) to aid in graphically displaying the spectra and wave properties (generating plots similar to those of Figures 8-16 and 19-23) are available from the authors and from the MVCO web site at <http://www.whoi.edu/mvco/data/data.html>.

Here we display, for the entire study period, statistical properties of the wind sea and the dominant swell system, together with the composite (MVCO and ASIT) wind record and the one dimensional form of the ADCP-derived wave spectra (Figures 19-23).

In viewing these graphs, one may partially assess the operation of APL-WAVES with our choice of parameters by considering how the wave field partitioning associated with a coastal storm changes in the storm’s passage. In simplest terms, one would expect the coastal wave field associated with a storm to develop and decay in two phases. As the storm winds actively force the local wave field, *i.e.* build a wind sea, one would expect the wind-sea wave height to grow with time while its dominant frequency declines. As the storm winds abate, the wind sea is essentially transformed to a swell system, which would be expected to decay in amplitude. Because wave group velocity is inversely related to frequency, the frequency of the incoming swell should tend to increase with time, as the higher frequency waves arrive later than the more rapidly traveling lower frequency waves.

For a “simple” storm, with single periods of growing and abating winds, APL-WAVES should then transfer the designation of a wave system from a wind sea to a swell near the point in time when the frequency of the wave system is at a minimum and its amplitude is near a maximum. In most, but not all, such “simple” storm examples, APL-WAVES, armed with our chosen parameter set, performs well according to this criterion. Consider, for example, the storm events of year-days 228-229 (Figure 19), 246-247 (Figure 20) and 293-294 (Figure 21). The building wind sea on day 294 also provides reassurance that use of the deep water dispersion relationship does not unduly affect the results. As the wind builds from 8 to 15 m/s on day 294 the wind sea is consistently identified even as the wind-sea period increases from 4 to 8 s, well beyond the deep water limit of about 5.8 s (Section 3a).

Despite the encouraging performance of APL-WAVES partitioning for “simple” storms, it is not rare for a building sea (*i.e.*, a sea with increasing wave amplitude and declining average

frequency) to be designated for some time of its development as a swell system. This often occurs later during the wave system development and is associated with a broadening rift between the directions of the wind and the peak of the wave system. In most instances, the difference between wind and wave peak direction is large enough to put the wind system peak out of reach of the wind-sea parabola, even for a wind-sea multiplier of 1.9. This difference is sometimes due to a shift in wind direction not matched by a corresponding shift in peak wave direction; and is at other times due principally to a shift in peak wave direction. Addressing this issue is beyond the scope of our project.

There are also frequent instances when the APL-WAVES designation of a wave system changes rapidly between wind sea and dominant swell. This behavior is particularly evident when the wind and swell directions are aligned in direction (e.g., Figure 19, days 217–220). This may occur due to a brief decline in wind speed, putting the wave system peak outside the wave parabola, or may be due to a spike in wind speed extending the parabola to the peak of a swell system. While such rapid redesignation of a wave system complicates the wave property time series produced by APL-WAVES, it is not necessarily an indictment of the program. Certainly, a swell can be actively driven by a sufficiently strong wind, and a wind sea can take on the properties of a freely propagating swell during a temporary lull in the wind.

Further complicating the interpretation of the MVCO wave observations is the complex geography of the MVCO region (Figure 1). The site is exposed to the open ocean to the south, but surrounded by Martha's Vineyard to the north, Nantucket Island to the east and the New England coastline to the west. As expected, swell was predominantly from the south. The proximity of the site to Martha's Vineyard results in short fetch (~20 km) for winds from the west and very short fetch (3–10 km) for winds from the north to east-northeast. Overall, the island shelters the site (limits wave fetch) for winds from about 260° to 75°.

Using the wind-sea properties produced by APL-WAVES for the period of 16–28 August 2003, during which persistent winds were from 180°–270°, Plueddemann (2006) found the strongest wind seas to be tightly clustered between 180° and 245° T. The interpretation was that a small island and various shoals to the southwest of Martha's Vineyard significantly limit wave development for wind directions between 245° and 270°. The evolution of these fetch-limited waves, as well as those for winds from the north and northeast, are a subject for future study.

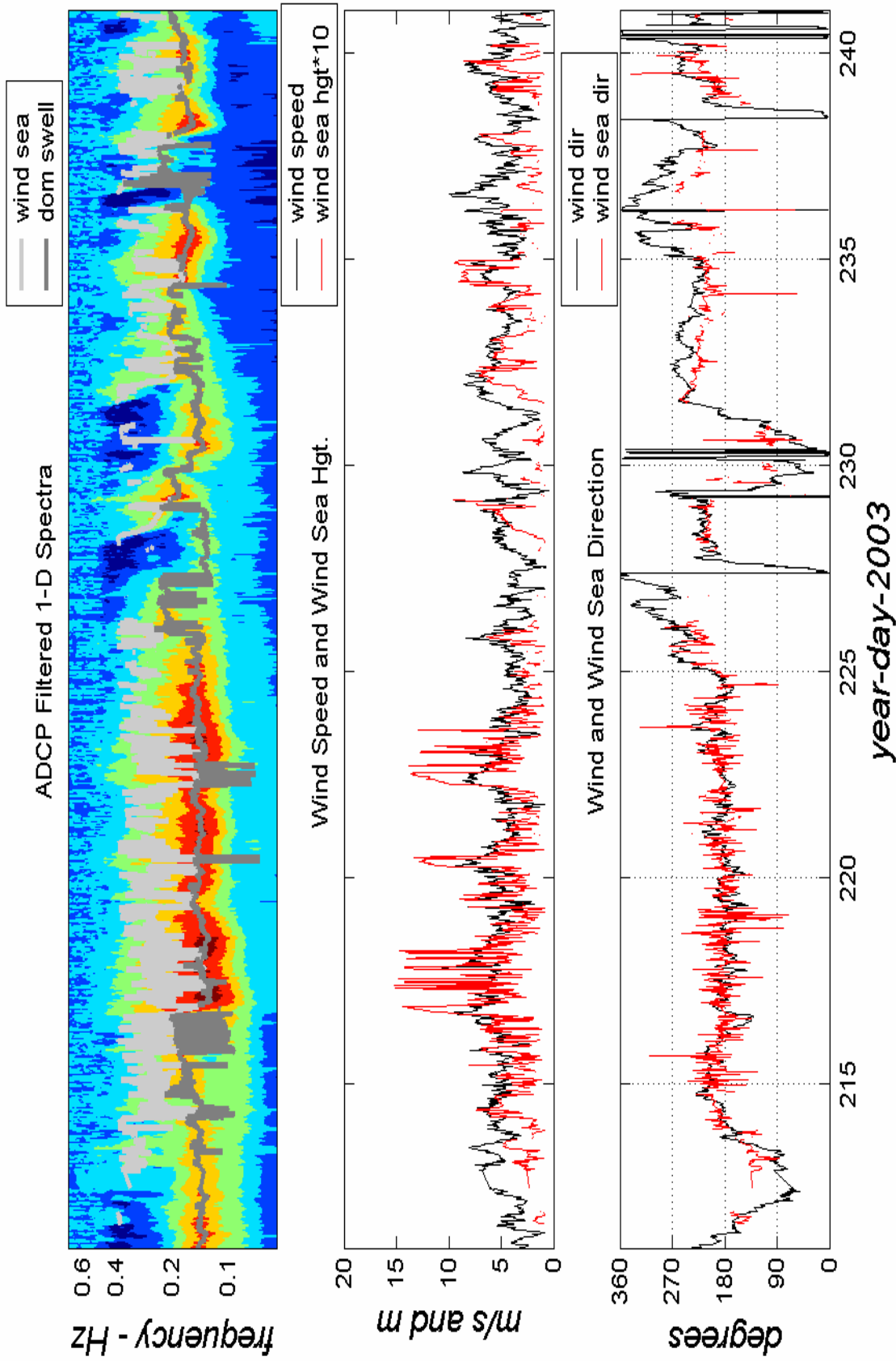


Figure 19. Subset of wave properties computed by APL-WAVES with parameter set g (Table 2) for the 30 day period from year day 211-240. Also shown are the one dimensional ADCP-derived wave spectra and the wind speed and direction.

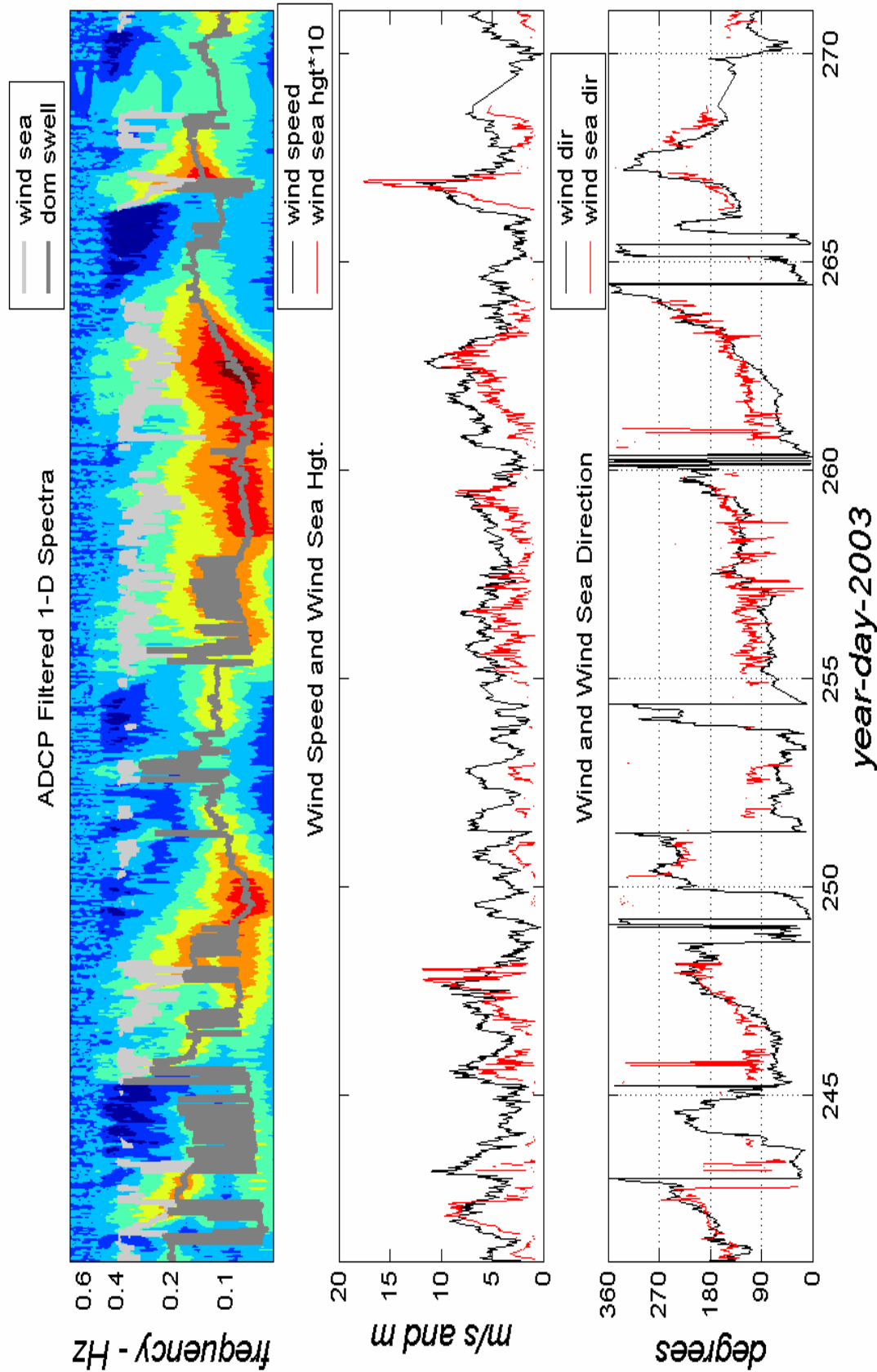


Figure 20. Same as Figure 19 except for year days 241-270.

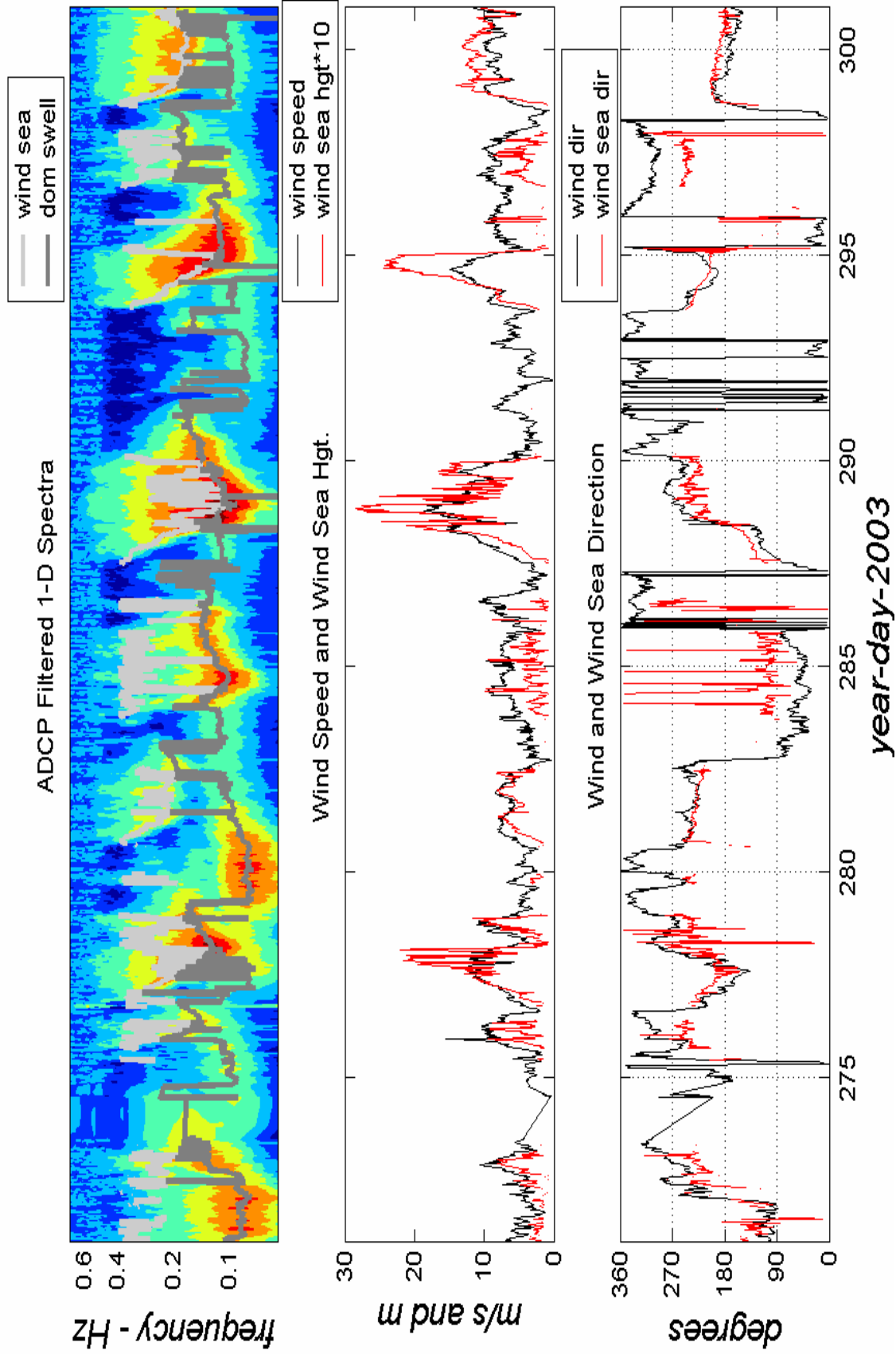


Figure 21. Same as Figure 19 except for year days 271-300.

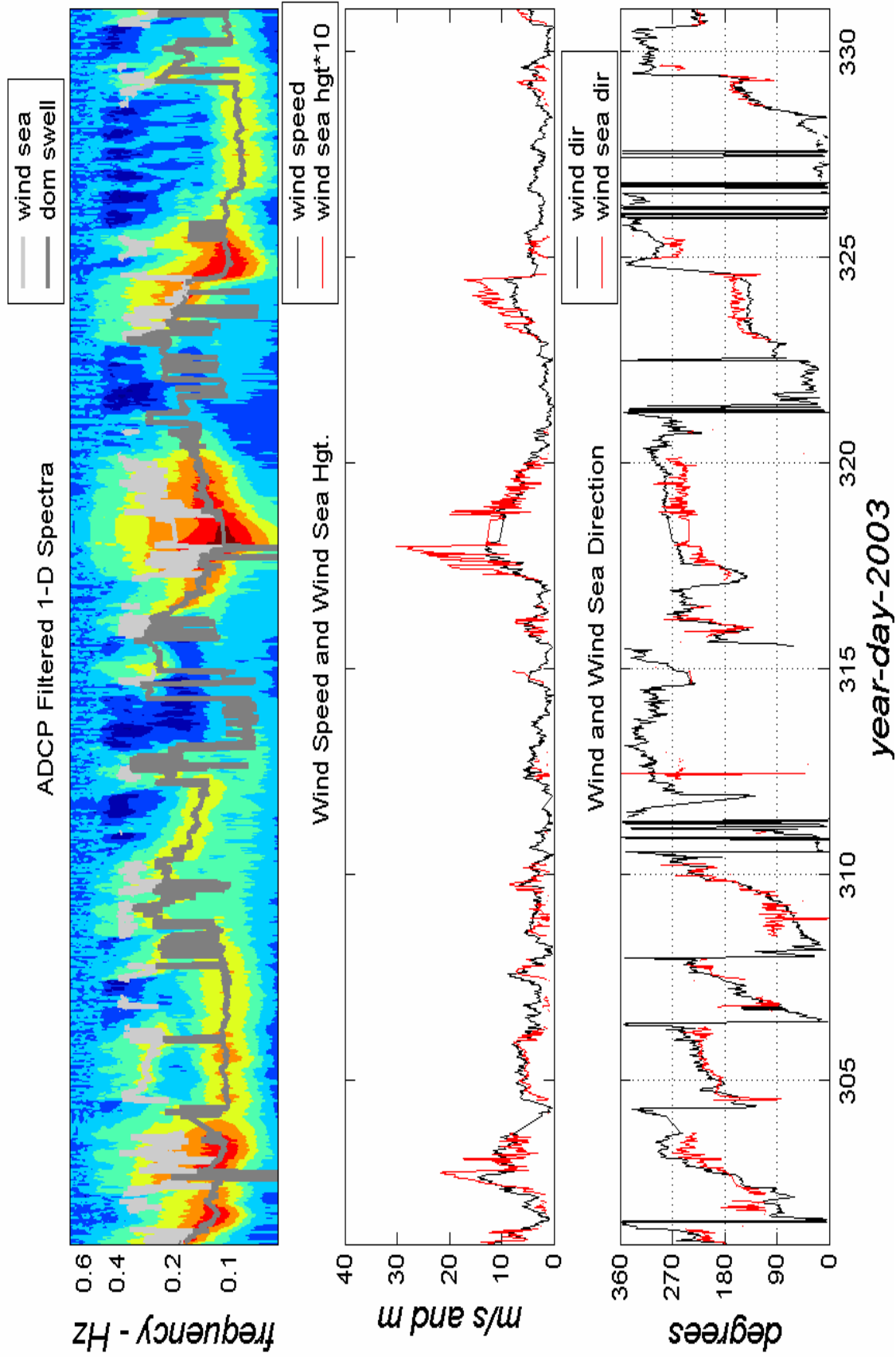


Figure 22. Same as Figure 19 except for year days 301-330.

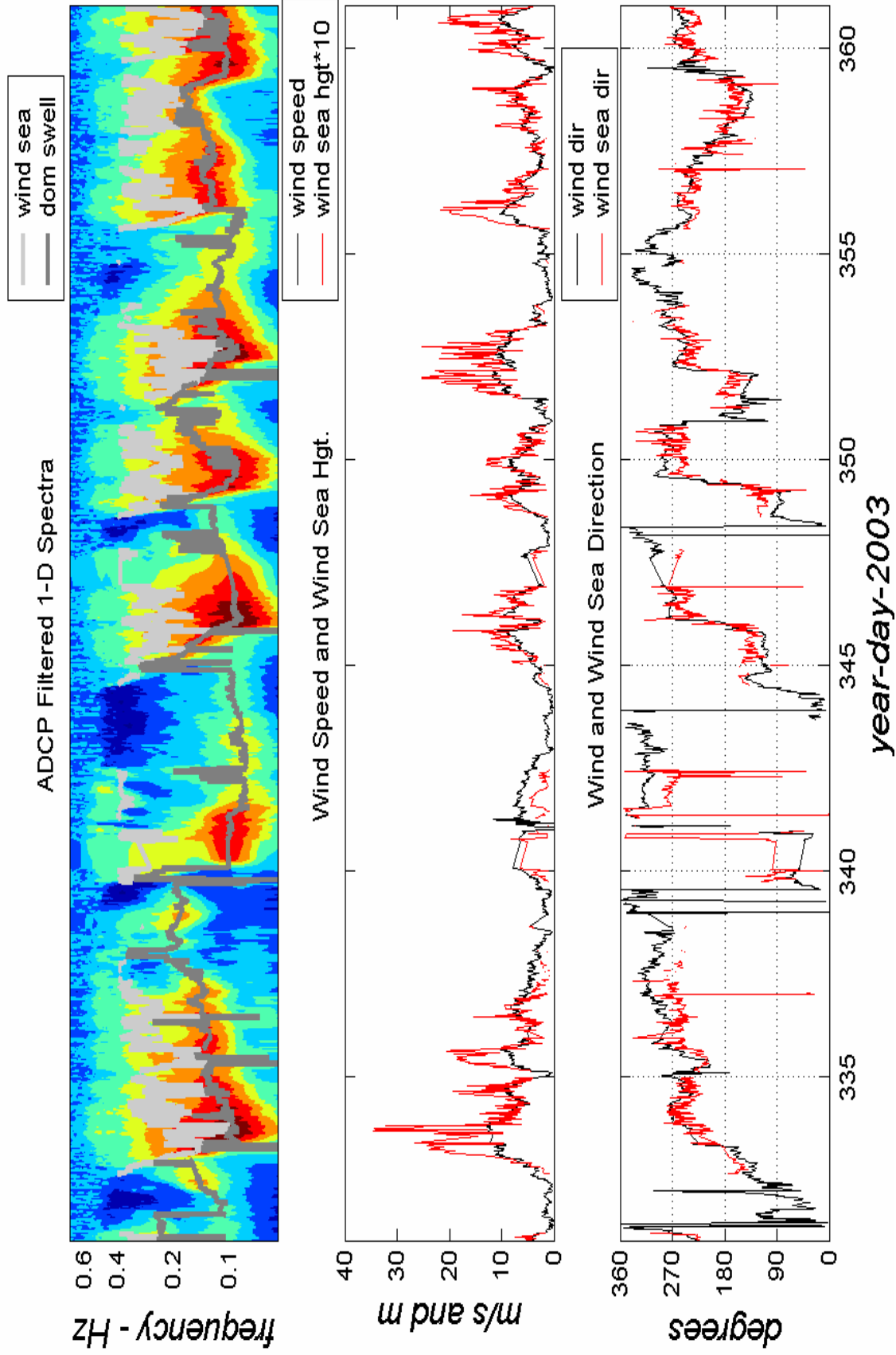


Figure 23. Same as Figure 19 except for year days 331-360.

Acknowledgments

The efforts of Jim Edson and support from the National Science Foundation were critical to establishment of the MVCO. The efforts of John Trowbridge and Jim Edson, and support from the Office of Naval Research were critical to establishment of the ASIT. Many on the Woods Hole Oceanographic Institution (WHOI) technical staff contributed to successful MVCO and ASIT observations. Marga McElroy provided field support and coordinated the connection of instruments. Ed Hobart specified hardware, operating system and support programs and wrote data acquisition/control software. The WHOI dive team installed and maintained the MVCO ADCP. Janet Fredericks produced the ADCP directional spectra using WavesMon. This analysis was funded by the Office of Naval Research under Grant No. N00014-03-1-0681 to the Woods Hole Oceanographic Institution.

References

- Austin, T.C., J.B. Edson, W.R. McGillis, M.Purcell, R.A. Petitt, Jr., M.K. McElroy, C.W Grant, J. Ware and S.K. Hurst (2002) A network-based telemetry architecture developed for the Martha's Vineyard Coastal Observatory. *IEEE Journal of Oceanic Engineering*, 27(2), 228-234.
- Edson, J.B., W.R. McGillis and T.C. Austin (2000) A new coastal observatory is born. *Oceanus*, 42, 31-33.
- Hanson, J.L. and O.M. Phillips (2001) Automated analysis of ocean surface directional wave spectra. *Journal of Atmospheric and Oceanic Technology*, 18, 277-293.
- Krogstad, H.E., R.L Gordon and M.C. Miller (1988) High-resolution directional wave spectra from horizontally mounted acoustic Doppler current meters. *Journal of Atmospheric and Oceanic Technology*, 5, 340-352.
- Plueddemann, A.J. (2006) Wind, waves and Langmuir circulation during CBLAST-Low, 27th Conference on Hurricanes and Tropical Meteorology, Monterey, CA, American Meteorological Society, CD-ROM, 7C.4.
- RØrbaek, K. and H. Anderson (2000) Evaluation of wave measurements with an acoustic Doppler current profiler. *OCEANS 2000 MTS/IEEE Conference and Exhibition*, Providence, RI, USA, Volume 2, 1181-1187.
- Strong, B., B. Brumley, E.A. Terray, and G.W. Stone (2000) The performance of ADCP-derived wave directional spectra and comparison with other independent measurements. *Proceedings Oceans 2000*, IEEE Press, 1195-1203.
- Terray, E.A., B.H. Brumley and B. Strong (1999) Measuring waves and currents with an upward-looking ADCP. *Proceedings IEEE 6th Working Conference on Current Measurement*, IEEE Press, 66-71.

Appendix 1: Description of Output Variables

The following wave field variables, representing the output of spectral partitioning described in Section 4b, are found in the MATLAB Ver. 6.5 file “wave_statistics.mat”.

Variable	Description	Units
ydstat	decimal year day of 2003 (noon on Jan 1 is day 1.5)	
parameters	character array describing APL-WAVES input parameters	
time	MATLAB serial date number	
windsp	10 m wind speed	[m/s]
winddir	10-m wind direction	[degrees true]
sighgt	overall significant wave height	[m]
peakper	period of overall wave spectrum peak	[sec]
peakdir	direction of overall wave spectrum peak	[degrees true]
windseahgt	significant wave height of the wind sea	[m]
windseaper	mean period of the wind sea	[sec]
windseadir	mean direction of the wind sea	[degrees true]
domswellhgt	sig. wave height of the dominant swell	[m]
domswellper	mean period of the dominant swell	[sec]
domswelldir	mean direction of the dominant swell	[degrees true]
secswellhgt	sig. wave height of the secondary swell	[m]
secswellper	mean period of the secondary swell	[sec]
secswelldir	mean direction of the secondary swell	[degrees true]

REPORT DOCUMENTATION PAGE	1. REPORT NO. WHOI-2006-13	2.	3. Recipient's Accession No.
4. Title and Subtitle Extracting Wind Sea and Swell from Directional Wave Spectra Derived from a Bottom-Mounted ADCP		5. Report Date July 2006	
7. Author(s) James H.Churchill, Albert J. Plueddemann, and Stephen M. Faluotico		6.	
9. Performing Organization Name and Address Woods Hole Oceanographic Institution Woods Hole, Massachusetts 02543		8. Performing Organization Rept. No.	
12. Sponsoring Organization Name and Address Office of Naval Research		10. Project/Task/Work Unit No.	
		11. Contract(C) or Grant(G) No. (C)N00014-03-1-0681 (G)	
		13. Type of Report & Period Covered Technical Report	
15. Supplementary Notes This report should be cited as: Woods Hole Oceanog. Inst. Tech. Rept., WHOI-2006-13.		14.	
16. Abstract (Limit: 200 words) Recent advances in processing velocity data from bottom-mounted Acoustic Doppler Current Profilers (ADCPs) offer the capability of partitioning directional wave spectra of surface wave height in order to separate locally generated wind waves from swell. In the study described here, we have partitioned directional wave spectra, derived from bottom-mounted ADCP measurements at the Martha's Vineyard Coastal Observatory (MVCO) south of Martha's Vineyard, MA, into dominant swell and locally generated wind-wave components. The partitioning was carried out following the method of Hanson and Phillips (2001) using an exploratory approach. As part of this approach, we assessed the validity of the ADCP-derived wave spectra by comparing them with one-dimensional wave spectra derived from laser altimeter measurements. This comparison identified a frequency range over which the ADCP-derived wave field may be suspect. We also carried out a series of sensitivity tests in which we evaluated how the results of wave partitioning according to the Hanson and Phillips (2001) method is influenced by varying the parameters required to implement the method. In this report, we describe and assess the data sources used in our study, outline the methods employed for wave spectra partitioning and describe partitioning results.			
17. Document Analysis a. Descriptors surface waves directional spectra spectral partitioning b. Identifiers/Open-Ended Terms c. COSATI Field/Group			
18. Availability Statement Approved for public release; distribution unlimited.		19. Security Class (This Report) UNCLASSIFIED	21. No. of Pages 41
		20. Security Class (This Page)	22. Price